Hydro-mechanical constraints and premonitory factors of landslide dam failure caused by seepage

浸透による地すべりダム崩壊の水力学的制約及び前兆現象

Dhungana Prakash

Feb. 2020

Hydro-mechanical constraints and premonitory factors of landslide dam failure caused by seepage

浸透による地すべりダム崩壊の水力学的制約及び前兆現象

Dhungana Prakash

S179842

A dissertation submitted in fulfillment of the requirements for the degree of

Doctor of Philosophy

Main Supervisor:

Prof. Fawu Wang, PhD

Department of Earth Science

Interdisciplinary Graduate School of Science and Engineering

Shimane University, Japan

Feb. 2020

Abstract

Landslide dams inevitably demonstrate the potential for catastrophic failure with high-risk damage to life and property at the downstream site. The formation of a landslide dam is a natural process; thus, minimizing the risk due to its failure is important. Landslide dam failure can be categorized into three types: seepage failure, overtopping and slope failure. As described by other researchers, the established premonitory factors of landslide dam failure are hydraulic gradients, seepage, and turbidity as well as vertical displacement and inflow rate into the reservoir. Knowledge of the internal instability of dam material is the key factor to predict the seepage failure of the landslide dam. Failure time is another factor to reduce the adverse effect of catastrophic floods. The objective of this study is to support field engineers for predicting the failure time of the landslide dam caused by seepage, based on the possible available data in the field without disturbing the dam body.

An experimental study has been conducted with a different mix of silica sand for failure and not failure cases to find the possible condition for dam crest failure and its stability. Three groups of samples that represented fine, medium and coarse particle sizes were prepared by Silica sand S4, S5, S6, and S8 of different proportions. These samples were used to conduct the flume experiments of failure and not failure cases. Premonitory factors of landslide dam failure behave differently in different particle size samples. From the experiment, it is found that the TSS trend line may be the initial factor for checking the stability of a dam crest. A landslide dam with an increasing TSS order will fail and a decreasing order may not fail. Based on all experiments, it can be concluded that the hydraulic gradient has three stages: 1) it starts to increase and reaches a peak value; 2) it starts to decrease from the peak value and reaches a minimum, and 3) it starts to

increase again where the seepage water begins to come out and the vertical displacement starts to increase. Dam failures always occur when seepage water comes out with an increasing TSS and increasing vertical displacement. Repeated experiments on samples having more fine particles show that if a landslide dam is formed by fine particles, then there would be a high chance of its failure. In the case of a constant hydraulic gradient, the landslide dam would be stable whenever there is an increasing vertical displacement and presence of TSS. Similarly, in case of constant vertical displacement and a decreasing TSS, a landslide dam would be stable.

Extensive laboratory work was done with mixed samples of silica sands to find the relation between seepage water volume and TSS. Seepage water was collected from a flume tank with the facility to measure the hydraulic gradient, vertical displacement, and seepage water volume. Grain size affected the life span of the dam. The seepage volume increased with the increase in the percentage of silica sand S4, whereas TSS increased with the increase in the percentage of silica sand S8. With the increase in the reservoir size with constant quantity of inflow, TSS decreased, and the total seepage volume increased.

Dam failure depends on the particle size, dam geometry, inflow rates, reservoir size, hydraulic gradient, and seepage water volume, and TSS of seepage water. Results indicated that with the increase in fine particles, the life span decreases, and TSS increases. With the increase in the inflow rate into reservoir, the dam life span decreases, and the TSS and seepage volume rate increase. With the increase in the reservoir size, for a same quantity of inflow, the total seepage water volume decreases.

These experiments of flume tanks provide a framework for a better understanding of the possibility of seepage-induced failure of landslide dams. The results of this comprehensive

research would aid in the development of accurate dam breach models and these results can be used in the field to predict possible failure time, which can reduce the disaster.

Acknowledgement

The thesis entitled "*Hydro-mechanical constraints and premonitory factors of landslide dam failure caused by seepage*" is written in order to fulfill the partial requirement for the degree of doctor in Department of Earth Science, Interdisciplinary Faculty of Science and Engineering, Shimane University, Japan.

First and foremost, I would like to express my deepest appreciation to my enthusiastic supervisor, Professor Fawu Wang, for his continuous guidance, support, and encouragement throughout my Ph.D. study in Shimane University. His immense ideas, suggestions, and patience give me endless power to overcome difficulties confronted during the research. His tremendous knowledge and positive attitude towards life and research will be lifelong benefits for me. It was really a great pleasure and privilege for me to be supervised by him.

I wish to express my sincere gratitude to all the professors and staffs in Shimane University, for their academic support and kind help in my Ph.D. study. The "lunch talk" organized by the Department of Earth Science and the field school organized by the International Student Section make my study and life in Japan more colorful and enjoyable.

I am grateful to all members of my dissertation committee for their time on the review and evaluation during the application. The valuable comments and suggests from the dissertation committee are of great help to improve the quality of this thesis.

Many thanks to my Ph.D. fellows, especially all my colleagues in "Swansliders group" from Professor Fawu Wang's laboratory in Shimane University for their kind support during this research. I would like to thank Dr. Zill Dai, Dr. Ji Feng, Dr. Zhang Shuai, Mr. Yoshiharu

Yokota, Mr. Kounghoon NAM, Ms. Ran Li, Mr. Akinori Iio, and Ms. Rong Zhou. The life, the field works, the seminars and the conferences we shared together will be lifelong reminiscence.

I would like to thank to the Izumo South Rotary Club as Sewa club, for providing me Rotary Yoneyama Memorial Doctoral Course Scholarship. I also would like to thank International student section of Shimane University for providing enormous support to find the scholarship.

I want to extend my appreciation to my family: my parents and relatives for moral supports and inspiration throughout my study period.

Last but not the least I am grateful to my dear wife *Sabitri Adhikari* who is a real blessing in my life. My study would not be possible without her unconditional support and courage. I am equally thankful to my kids *Anushri* and *Ankur* for fulfilling each day with eternal happiness and joy.

Table of content

List of tables

List of figures

CHAPTER 1

Introduction

1.1 Background

Construction of human facilities and change in environment and global warming continuously affect the hydrogeological system all around the world. The intensity and extremely high temperatures are increasing in the last two decades. These effects have prompted several natural disasters including landslides and landslide dams and glacier-ice dams. The relation of climate change and initiation of several mass movements have been studied in many literatures (Bo et al, 2008; Jakob and Lambert, 2009; Crozier, 2010; Stoffel and Huggel, 2012).

A landslide dam refers to blockage the water channel by sliding, flows and avalanches, which is common in geo-hazard for earthquake prone area and heavy rainfall precipitation area (Costa and Schuster, 1988; Canuti et al., 1998; Ermini and Casagli, 2003; Korup et al., 2010; Tacconi et al., 2018). A landslide dam is formed by the heterogeneous mass of unconsolidated or poorly consolidated earth and rock materials and has no engineering supports such as filters, drainage, support wall, etc., so it has a high potential of failure with the catastrophic flood to the downstream side. Similarly, landslide dam may cause the flooding of upstream area with high risk of submergence. For the catastrophic failure of landslide dam, it has to predict the resulting outflow hydrograph in order to determine flooding area and hazards in the downstream side. Therefore, failures of landslide dam have been, and continue to be, the subject of numerous studies attempting to define processes, risks and mitigate measures (Costa and Schuster, 1988;

Costa and Schuster, 1991; Schuster, 2000; Manville, 2001; Ermini and Casagli, 2003; Korup, 2004, 2005).

A few examples of the earliest historical records of landslide dams formation and failure are: in the European Alps include the 1219 damming of the Romanche River in France and failure of dam led to the downstream flooding that claimed thousands of lives (Bonnard 2011). The 1419 Ganderberg-Passeier Wildsee (Passer Valley, Italy) rockslide dam failure and outburst flood that claimed at least 400 lives; and the 1515 Val Blenio (Switzerland) rock avalanche dam failure and outburst flood that took about 600 lives (Li, 1990). In China, the 1737 BC earthquake-triggered landslide dam in the Yi and Lo Rivers in Hunan Province of central China. The 1786 (M = 7.75) earthquake-triggered landslide in Sichuan Province, southwest China, which dammed the Dadu River and breached after ten days of formation, leading to catastrophic flooding of the downstream areas that claimed over 100,000 lives (Dai et al., 2005). For instance, the failure of three landslide dams (i.e., the Dahaizi, Xiaohaizi, and Diexi landslide dams) induced by the 1933 Diexi earthquake in China led to a loss of approximately 2500 lives. The potential failure of the Tangjiashan landslide dam induced by the 2008 Wenchuan earthquake in China threatened more than 1.3 million people in the downstream areas (Liu et al., 2009).

Landslide dams have high risks due to its potential of catastrophic outburst floods with huge amount of flow of hyper-concentrated peak discharge, which threaten the lives and property of people to the downstream areas (O'Connor and Costa, 2004). Peak discharges are controlled by several factors including dam geometry, downstream topography, and failure mode, the internal structure of the blockage and lake volume. Therefore, a good knowledge of the complex processes involved in the evolution and failure of river- damming landslides, coupled with the hydraulics of the outburst floods, is essential for disaster risks assessment and mitigation.

History of failure cases insight that the chance of the loss of life due to a dam failure depends upon the warning time available to evacuate from the downstream risky area (Dekay and McClelland, 1993; Jonkman et al., 2008). The warning time depends on the failure mode and the erosion resistance of the dam materials. Therefore, it is important to study the failure mechanisms of landslide dams and simulate the dam breaching process.

Internal erosion can occur whenever soil is exposed to a potentiometric gradient. Internal erosion occur in many geologic materials including clay, silt, fine sand, volcanic ash, tuff, loess, colluvium, alluvium, claystone, siltstone and mudstone (Parker, 1964). Internal erosion in soil can be initiated by concentrated leak erosion, backward erosion, contact erosion, or suffusion (Fell and Fry, 2007). Generally, internal erosion depends upon the seepage volume and grain size distribution of landslide dam material.

Failure of landslide dams and earthen dams involves a complex, sporadic, nonlinear and homogeneous process (Singh et al., 1988). Hence, a good knowledge of soil particle transport processes, including the hydraulics and hydrodynamics is required for a better understanding of the complex processes that lead to internal erosion. Assessment of landslide dams and prediction of the flood hydrograph are essential for effective planning and implementation of disaster management schemes. Similarly, a large number of results abound on numerical models developed for the simulation of piping in earthen dams and landslide dams (Singh et al., 1988; Gattinoni and Francani, 2009). Similarly, Wang et al., 2018; Okeke et al., 2016a, 2016b; and many more studied about the internal structure and piping failure. Yet, none of these methods have investigated the influence of hydro-mechanical properties of landslide dams on failure or for not failure case of landslide dam. After the formation of landslide dam, due to remote location and risk of failure, there will be always limited data to predict the failure time, so it is

important to find the inter-relationship among these available data for failure and stability of the dam.

1.2 Research objectives and thesis outline

The purpose of the present research is to study the hydro-mechanical constraints and premonitory factors of landslide dam for failure and not failure cases considering the seepage failure. This thesis is focused on the following main objectives.

- Finding the difference of failure and not failure condition of landslide dam in terms of premonitory factors of landslide dam failure and seepage water.
- Finding the relation of total suspended solids (TSS) for different mix of silica sand and condition of TSS for failure and not failure cases
- Prediction of failure based on hydraulic gradient, vertical displacement and TSS.
- To study the effects of dam height, reservoir size and material on seepage volume and TSS for seepage failure of landslide dam.

These objectives are achieved through the series of experimental studies in a flume tank equipped with monitory sensors, seepage water collection facility and using different mix of artificial silica sand of different grades.

This thesis is focused on the theme of understanding the relationship among the premonitory factors of landslide dam failure caused by seepage failure and the relation between seepage water and TSS of landslide dam failure.

Chapter 1 reviews previous research on the landslides dam failure and importance of study and objective of the study

Chapter 2 describes brief discussion on failure mechanism and hydro-mechanical constraints and premonitory factors of landslide dam failure.

Chapter 3 presents the methodology of this study. In this chapter, experimental setup and material used and procedure of experiment have been discussed.

Chapter 4 presents the relationship among the premonitory factors of landslide dam failure caused by seepage.

Chapter 5 presents the relationship between seepage water volume and total suspended solids of landslide dam failure caused by seepage.

Chapter 6 concludes the thesis by highlighting several findings of the experimental studies on landslide dam failure caused by seepage, understanding for the prediction of landslide dam failure at site level from the available data sets.

CHAPTER 2

Literature review

2.1 Formation and failure of landslide dam

Landslide dam can form in a wide range of physiographic settings and topography, from high alpine debris avalanches to quick-clay failures in wide valley floors. Landslide dams are formed by various kinds of landslides, ranging from rock falls and rock slides in steep walled, narrow canyons to earth slumps in flat river lowlands (Costa & Schuster, 1988; Schuster, 1995). From the historical landslide dam data, set of 390 landslide dam, it is found that 40% were formed by rock and soil slumps and slides, 30% by debris, earth and mud flows, 25% by rock and debris avalanches and less than 10% by sensitive-clay failures and rock and earth falls (Shuster, 1995). The most common mechanisms triggering dam-forming landslides are excessive precipitation (58%), and earthquakes (33%). The highest of historic landslide dam is 600m, which was earthquake induced Usoi rock-slide dam in southern Tajiskitstan, which forms 500m deep Lake Sarez. The direct and indirect cost due to landslide dam may be very high. The total costs (direct and indirect) of large debris slide at Thistle, Utah, were probably on the order of $400 million. Although there were no casualties as a result of the Thistle slide, it ranks as the most economically costly individual landslide in North America, and probably in the world (Schuster and Highland, 2001). According to worldwide statistics (Costa and Schuster, 1988) 27 % of landslide dams (n = 73) fail within one day of formation, 41 % within one week, 56 % within one month, and 85 % within one year. Landslide dam may fail by different failure mode based on material properties of the dam body and stream channel conditions. It may fail by the erosive

destruction due to overtopping, abrupt collapse of the dam body or progressive failure (Takahashi, 1991). Landslide dam most commonly fail by overtopping, followed by breaching from erosion by the overtopping water. Based on study of actual landslide dam failure, it seems more than 51% of failure cases were due to overtopping and failure mode of more than 48% cases were unknown (Schuster and Costa, 1986). The overtopping of water and the associated erosion of the dam body cause the majority of failures. A few examples are due to piping or sliding collapse of the dam body.

2.2 Failure mode and longevity of landslide dam

The failure mode of landslide dam is very similar to that observed for artificial earthen dams, generally occurring by overtopping, and infrequently by piping or slope failure or internal erosion (Costa and Schuster, 1988). Peng and Zhang (2012) made a comparison of failure modes of landslide dams, earth and rock fill dams using the datasets of 144 landslide dam failures, and 176 earth and rock fill dam failures. The result of their analysis indicated that 37% of piping cases were recorded in fabricated earth and rock fill dams while 8% were recorded in landslide dams (Figure 2.1).

The life spans of most landslide dams are relatively short. Nearly 50% failed within one week and 80% within one half year. The life span depends on the inflow into the dammed lake and the geotechnical properties of the dam materials (e.g., erodibility of the dam material, shear strength) and geometry of landslide dam. Thus, it is essential to predict the failure process of landslide dams originating from geotechnical considerations.

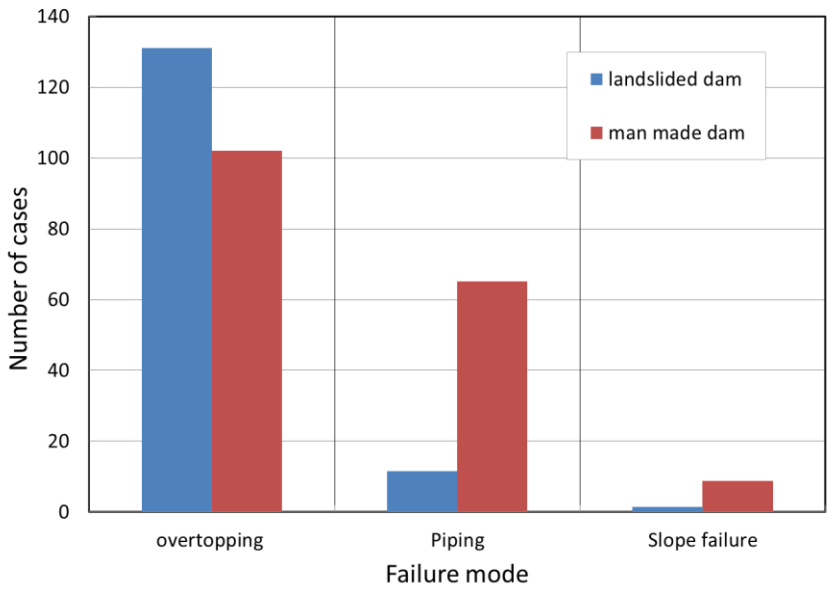

Figure 2.1 Comparison of failure modes of landslide dams (144 cases) and man-made earth and rock-fill dams (176 cases) based on historical cases inventoried by Peng and Zhang (2012)

In general, the development of internal erosion and piping in their early stages is not usually visible, but manifests when the internal erosion process has progressed towards an unprotected exit. The vulnerability of landslide dams to internal erosion and piping has been attributed to their heterogeneous nature, unlike engineered earthen dams which have undergone systematic compaction or have seepage barriers to reduce the potentials for internal erosion.

2.3 Significance of landslide dam in Japan and Nepal

2.3.1 Landslide dam in Japan

The geologic and geomorphic features of Japan are continuously changing due to the movement of pacific plate and Philippine Sea plate, which result frequent natural disasters including, earthquake, volcanic eruptions, typhoon. Landslides, debris flows, and catastrophic outburst

flood are common resulting disasters in japan (Sassa, 1998, 2005; Chigira and Yagi, 2006; Hayashi et al., 2013). The occurrence of landslide dams in several part of the Japanese Islands has been attributed to the abundance of steep and unstable mountain slopes with average modal angle of 35º (Katsube and Oguchi, 1999), high-gradient streams, narrow gorges, coupled with frequent hydrologic and seismic events (Swanson et al., 1986; Oguchi et al., 2001).

The October 23, 2004, Mid Niigata Prefecture earthquake (Mw=6.8) triggered thousands of landslides. At that time, 30 small-scale landslide dams were formed in the Imogawa River and its tributaries (Chigira and Yagi, 2006). These landslide dams were breached in short life span of several hours. Their short lifespan has been related to the materials forming the dams that were mostly comprised of highly weathered bedrock and regolith (Wang et al., 2007). However, emergency countermeasure works (construction of spillways, water diversion pipes/tunnels, and installation of drainage with 12 pumps) were carried out on the Terano and Higashi-Takezawa landslide dams to avoid potential dam breaching (Sassa, 2005).

In 2011 September, Typhoo Talas hits the southern part of Kii Peninsula, and concentrated rainfall was recorded maximum 2436 mm in 5 days in some area of Nara prefecture. About 207 landslide, landslide dams, debris flows and other sediment related disasters were recorded, among them 17 landslide dams were formed in different locations. Five landslide dams were produced risk of failure due to the rate of increase in reservoir level (Fig. 2.2, Hayashi et al. 2013).

Based on the above studies and information, it can be concluded that Japan is regularly affected by earthquake, and heavy concentrated rainfalls which results the landslide and landslide dam. So, it is important to study the failure of landslide dam and its affect to downstream.

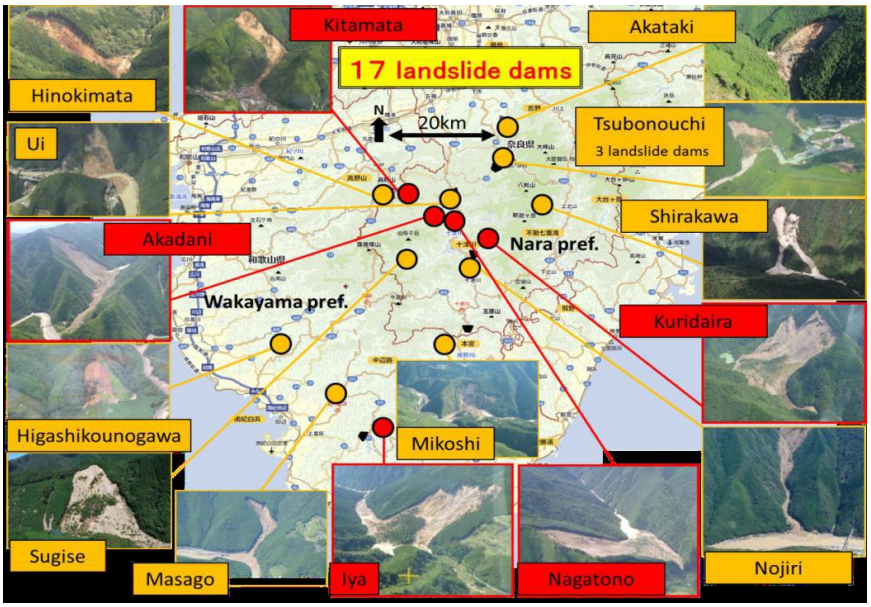

Figure 2.2 Distribution of 17 landslide dams triggered by Typhoon Talas in the Kii Peninsula. The images in red borders represent dams where emergency investigations were carried out (Hayashi et al. 2013).

2.3.2 Landslide dam in Nepal

Nepal is mountainous country rich in rivers. Rugged topography, unstable geological structures, soft and fragile rocks, common earthquakes, along with heavy and concentrated rainfalls during monsoon periods cause severe landslides and related phenomena in the Himalayan region (Dahal et al., 2008). The earthquakes of 1934, 1953, 1969, 1980 and 1988 triggered many landslides in Nepal (Dhital, 2002). Landslides in the Himalaya are scale-dependent, from massive extent of whole mountain ranges (gravity tectonics) through failure of single peaks to minor slope failures (Shroder and Bishop, 1998). More than 80% of the total annual precipitation occurs during the summer four months (June–September). Likewise, the distribution of daily precipitation during the rainy season is also uneven. Sometimes, 10% of the total annual precipitation can occur in a

single day and 50% of the total annual precipitation is often recorded within 10 days of the monsoon period. Such an uneven rainfall pattern is thought to play an important role in triggering landslides in Nepal (Dahal et al., 2008).

A massive landslide occurred at Jure village of Nepal on August 2, 2014. The landslide mass blocked the Sunkoshi River and created a landslide dam. Thirty-seven days after the formation, the Sunkoshi landslide dam breached on September 7, 2014. The peak flow discharge of the Sunkoshi landslide dam outburst at the dam outlet was found to be 6436 m^3/s, and the estimated time of the dam breach was found to be about 26 min (Shrestha and Nakagawa, 2016) (Fig. 2.3).

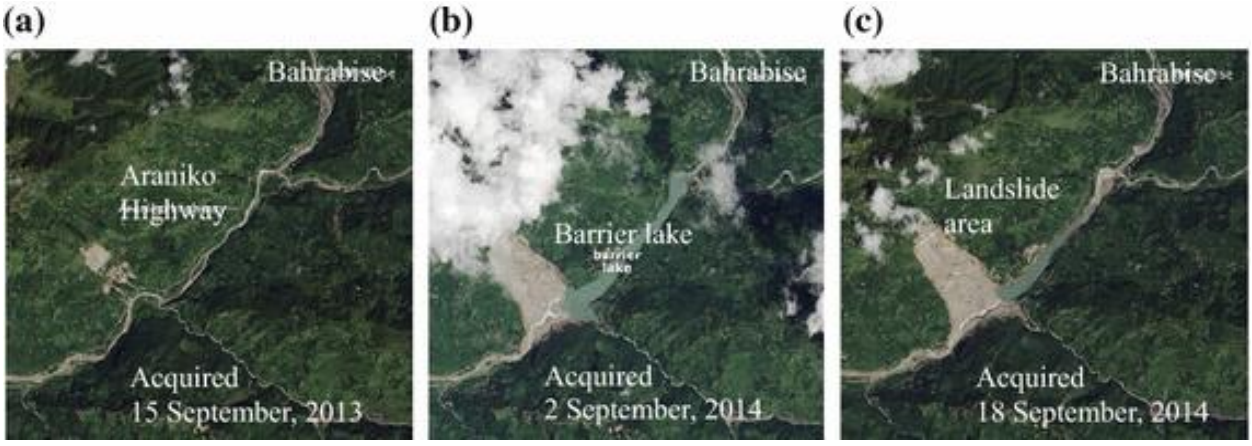

Fig. 2.3 Landsat 8 satellite images a) before landslide; b) after landslide and before landslide dam breach; and c) after landslide dam breach (Shrestha and Nakagawa, 2016).

So concentrated rain fall, time-to-time massive earthquake, geography and topography and history of Nepal shows the potentiality of landslide dam and its risk. Based on topography of Nepal, it can be categories as the most porn area for landslide formation, especially at the time of rainy season for mountainous area.

2.4 Internal erosion of landslide dam

Internal erosion initiated by suffusion is a progressive process and can induce the following incidents (Wan, 2006): (a) slope failure at the downstream face; (b) excessive settlement of the dam with loss of freeboard; and (c) formation of sinkholes at the crest and the upstream of the dam. In the first case, as the loss of the fine particles occurs at the seepage exist of the downstream slope, the local pore water pressure increases in addition to the decrease of shear strength of the soil. The slope stability is affected. Local slope failure may occur and the process then continues backward to the upstream. In the second case, due to the loss of fine particles within the core or filters, the coarse matrix may rearrange and the total volume decrease and the settlement occurs. In the third case, due to the loss of fine particles within the much permeable flow paths, the fine particles are washed away along these paths. Therefore, change of the volume of the coarse matrix occurs along these paths and a local sinkhole form.

As landslide dams are heterogeneous and mixed with boulders and shrubs, there may be interconnected large pores, due to which seepage from the dam could potentially lead to internal erosion/piping/seepage (Costa and Schuster, 1988). According to Dunning at al., 2006; Seepages have been noted on the downstream faces of many landslide dams, for example, the Tangjiashan landslide dam induced by the 2008 Wenchuan earthquake, the Cerro Condor- Sencca landslide dam failed in 1945 in Peru (Snow, 1964), and the Tsatichhu landslide dam failed in 2004 in Bhutan. Downstream slope failure of the Tsatichhu landslide dam has been observed due to the loss of fine particles under seepage flow, followed by overtopping failure. According to the literature (Glazyrin and Reyzvikh, 1968), the Lake Yashinkul landslide dam was known to have failed by internal erosion.

2.5 Mechanism of internal erosion for landslide dam

As the water level increase in the reservoir, the water starts to enter into the soil through the voids. At the same time, the total pressure head to the upstream and downstream side of the dam will be varying, and a force will be generated for seepage flow. As the interlocking bonding force of the soil matrix become smaller than the seepage force, it will start to erode the free fine particles, due to which enlargement of the seepage flow path will occur, and seepage force will be increased. The increased seepage forces start to break the interlocking bonding of soil particles and start to the erosion of unlocked particles. The erosion resisting forces depend on several factors including the plasticity index of the soil, the interlocking effect, gradation, cohesion, and the dispersive characteristics of any clay in the soil as well as the density of the soil particles (Singh, 1996).

The initiation of internal erosion by suffusion requires a soil particle has to detach from its parent material and become transported through sufficiently large voids and constrictions. Detachment and transport of soil particles require a hydrodynamic force against the intergranular friction. For internal erosion to continue, it requires large seepage forces to drag the relatively stable fine particles within the pores and large soil constrictions to permit further movement of the fine particles. During the suffusion process, the microstructure and the mechanical response of the soil change continuously.

When the seepage velocity is sufficiently large, particle mobilization caused by the drag forces exerted by the seepage flux causes undercutting and subsequently induces slope failure. Seepage can trigger erosion and instability in landslide dams and soil slopes through three interrelated mechanisms: (1) effects of pore-water pressure on the shear stress of the soil (2) increase in

hydraulic gradient forces acting on the soil, and (3) the detachment and entrainment of soil particles in the direction of the seepage flow (Fox and Wilson, 2010).

Once seepage process commonly occurs in landslide dams and soil, a slope is sapping. At that moment, seepage water exit from the downstream slope of landslide dam and streambanks under a sufficiently high hydraulic gradient induced by the seeping water (Hagerty, 1991). Sapping is usually initiated when exfiltration occurs over a wide area. Under favorable conditions, the process can intensify causing an increase in hydraulic gradient and subsequent erosion of the soil materials, shortening the seepage paths. This could potentially lead to undermining of the downstream slope and breaching of the dams once there is a sufficient supply of water (Zhang and Chen, 2006; Okeke et al., 2016a).

Howard and McLane (1988) have evaluated the conditions governing the mechanisms of seepage-induced transport in cohesion-less sediment. The authors carried out a series of experiments using a flume tank of dimension 2.5 m ×0.6 m ×0.051 m. Results of their experiments showed that three distinct zones occurred at the sapping face: the undermining zone, the sapping zone, and the fluvial zone. The majority of the hydraulic erosions were found to concentrate in the sapping zone, mostly characterized by steep surface gradients, intermittent shallow bulk failures and rapid upward seepage. Howard (1988) observed that seepage

2.6 Hydro-mechanical constraints

Understanding the internal structure and material properties of landslide dams is essential for evaluating their potential failure mechanisms, especially by seepage and piping. Recent research has shown that the behavior of landslide dams depends on the internal composition of the impoundment. The increment in the reservoir level directly affects the seepage force. The change

in pore water pressure can be recorded in laboratory, and hydraulic gradient can be calculated. Okeke et al. (2016b) use the Darcy law of flow to measure the hydraulic gradient of landslide dam in laboratory. Hydraulic gradient for two point of a dam can be computed as

$$i = (h_2 - h_1)/l \tag{2.1}$$

Where *i* is hydraulic gradient, h1, and h_2 are the total pressure head of upstream and downstream side respectively and *l* is the distance travel by the seepage water. From the above equation, the hydraulic gradient can be monitored continuously, if we have the pressure head of two points into the landslide dam. The pore water pressures not only support to understand the hydraulic gradient, it supports to know the seepage force applied for internal erosion.

2.7 Premonitory factors of landslide dam failure

Identifying premonitory factors before final failure for long-existing landslide dams is of importance step in disaster prevention and risk reduction. The probability of landslide dam failure remains an integral part of flood-risk modeling and hazard assessment studies. Costa and Schuster (1988) reported that the longevity of landslide dams depends on several factors including the rate of seepage through the dam; the internal structure and material properties of the dam; the size, shape, and volume of the blockage; and the rates of sediment and water flow into the upstream lake. Form the series of experimental studies (Wang et al., 2018), the interrelation of dam crest settlement, seepage water turbidity, self-potential method to measure water flow inside the dam body are the main premonitory factors that can be monitored in the field.

From the above, the process of failure and premonitory factors of landslide dam failure are determined without disturbing the dam structure. In the actual landslide dam, it is difficult to predict the hydraulic gradient and internal structure. The relationship among the premonitory factors of landslide dam failure and relationship of seepage water volume and TSS, which can be measured in the site, are helpful for the prediction of failure.

CHAPTER 3

Methodology

3.1 Experimental setup

In the laboratory, a flume tank with 0.45 m height × 0.45 m width × 2.0 m length was prepared for the experiment. On the downstream side of the flume tank, the flow of seepage water was stopped and diverted into a tank using holes at a distance of 0.75 m from the dam center. Experimental studies of the flume tank were performed for the selection of a dam size, including the 1 m × 0.6 m × 0.45 m model used by Sidle et al. (1995), 5 m × 0.3 m × 0.5 m model used by Awal et al. (2009), 1.5 m × 1 m model used by Wilson (2009), 1.4 m × 1 m model used by Wilson (2011), and 0.5 m × 0.5 m × 0.5 m model used by Fox et al. (2014).

In this study, experiment works has been conducted using the same flume tank for two different groups of samples prepared by mix of silica sand. Fig.3.1 and Fig. 3.2 are the flume tank setup for the experiments. Using the first setup (Fig. 3.1), the relationship among the premonitory factors of landslide dam failure caused by seepage was studied. Similarly using second setup (Fig.3.2), relationship between seepage water and TSS was studied.

In this study, the dam heights were 0.2 m and 0.25 m, and upstream and downstream slopes were 45° and 35°, respectively. The dam height was increased from 0.2 m to 0.25 m whereas the downstream and upstream slopes were constant, and the dam volume was also increased due to height increase. Similarly, in the flume tank, the position of the dam was shifted downstream side by 0.1 m to increase the reservoir size. The width of dam crest was 0.1 m. On the floor of the flume tank, a double-sided tape was used, and dry silica sand 6 was poured over it to

maintain the roughness between the dam material and flume tank floor. The flume tank was built using Plexiglas, permitting visibility into the flume. The flume bed slope was maintained constant at 1:40 during all experiments. Four pore-water pressure sensors, with a rated capacity of 50 kPa, were used—hereafter referred to as Pwp1, Pwp2, Pwp3, and Pwp4—for the downstream and upstream sides of the dam body and at the reservoir and seepage water collection tank, respectively. Sensors Pwp1, Pwp2, and Pwp3 were connected to the flume tank from the base of the flume tank facing upwards. The filter material to control the flow of sand over it covered Pwp1 and Pwp2. The Pwp4 sensor was connected to the tank base, where seepage water was collected. Multi-function analog laser sensors (CMOS) were used to measure the vertical displacement from the top of the flume tank using a wooden frame—hereafter known as Vdr and Vdl, for the right and left sides, respectively. The vertical displacement of the dam crest was continuously monitored at two fixed points by laser sensors. A half-cut polyvinyl chloride (PVC) pipe was fixed below the holes with a gentle slope to collect seepage water. The Pwp4 sensor monitored the collected seepage water volume.

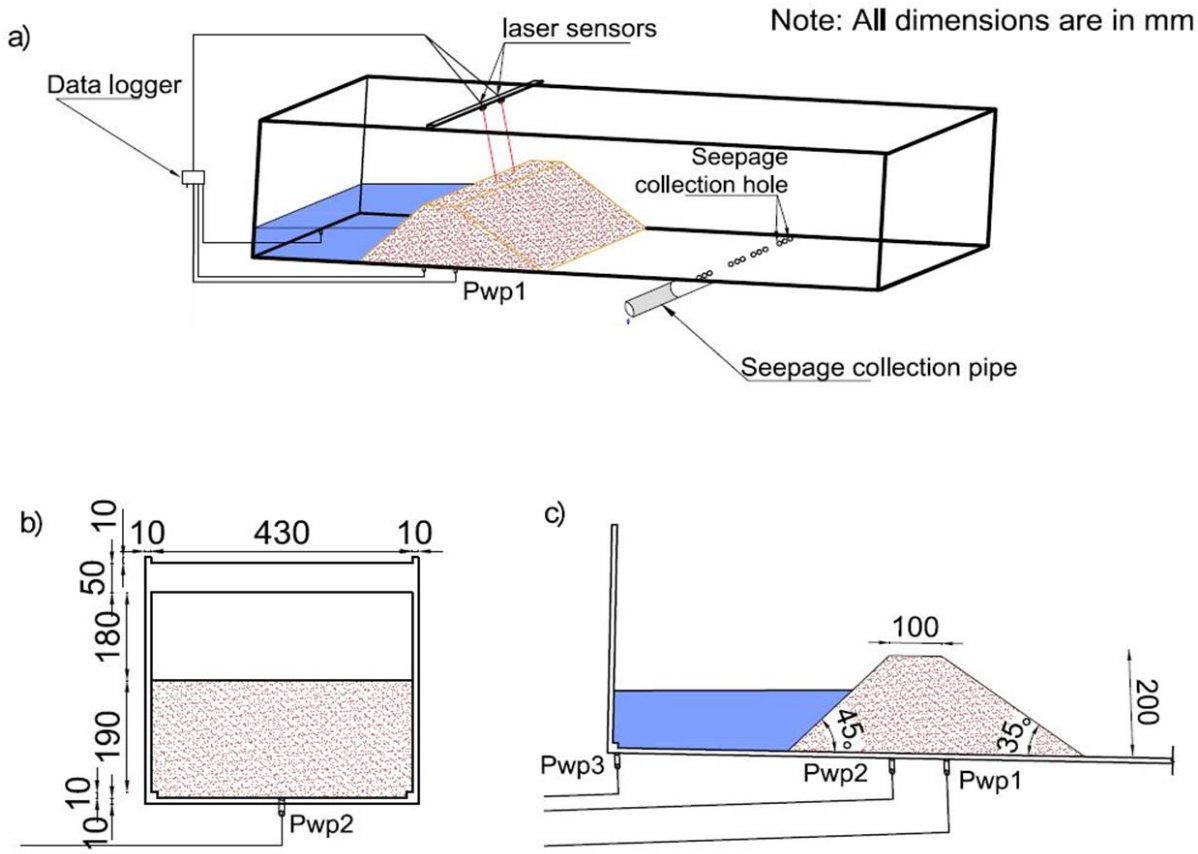

Fig. 3.1 Experimental setup of the flume tank for samples of Group A. a) 3D view; b) cross-section and; c) longitudinal section.

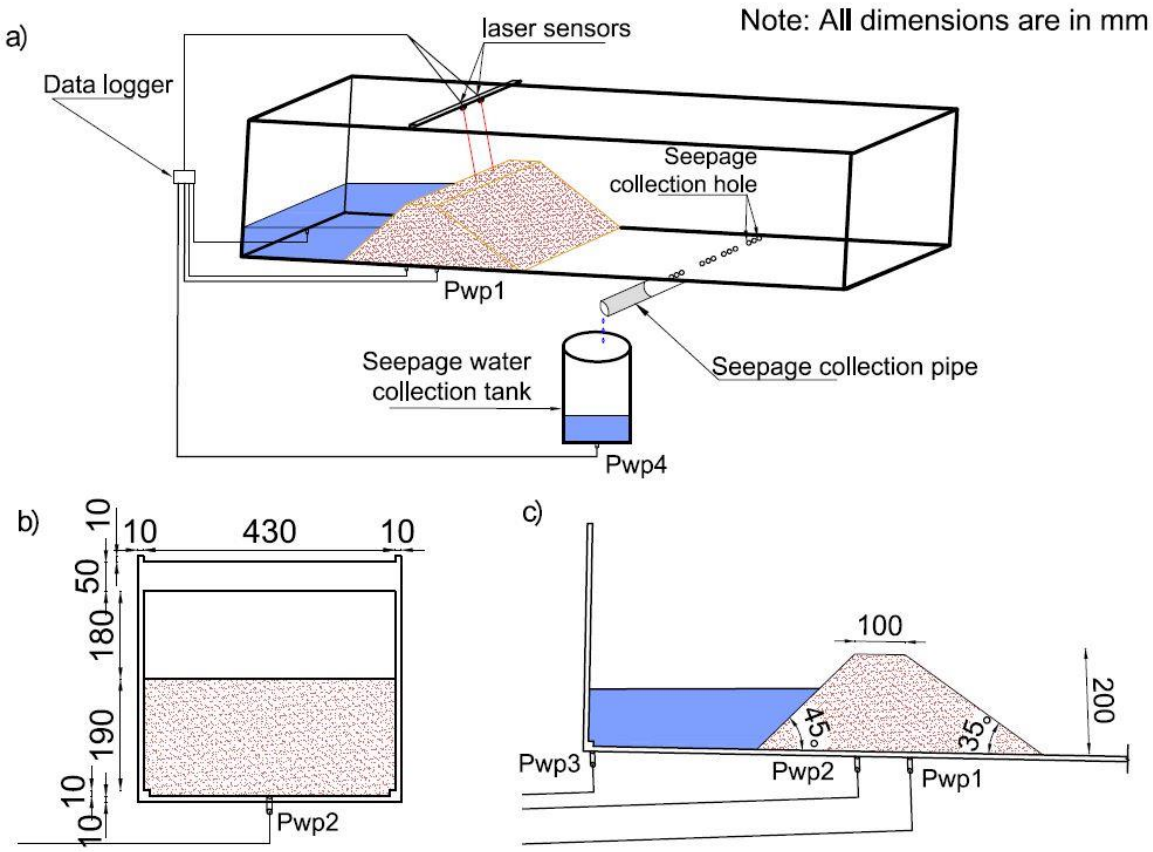

Fig. 3.2 Experimental setup of flume tank for samples of Group B. a) 3D view; b) cross-section; and c) longitudinal section.

3.2 Materials

Typically, landslide dams comprise fragmented materials with a wide range of sediment sizes (Costa and Schuster 1988; Schuster 1995). It is challenging to scale down actual landslide dam material to the laboratory scale. Artificial silica sand was selected as the sample and a combination of silica sand S4, S5, S6 and S8 were used in different proportions, as shown in Table 3.1 for the relation among the premonitory factor of landslide dam herein after called Group A sample.

Before conducting the final experiment, a series of experiments were performed for selecting the sand mix ratio and initial water content for creating the desired dam shape. Silica sand is artificial sand but, in the field, the presence of different soil minerals plays a vital role in grain size percentage and turbidity. Kaolinite, which is one of the soil minerals present in most natural soils, was used here to understand the effects of minerals on seepage water, hydraulic gradient and vertical displacement. Silica sand S5 and S6 were considered to be the main dam material constituents and silica sand S4 and S8 played the role of coarse and fine particles, respectively. Based on this, samples SAM1, SAM2 and SAM5 had more fine particles i.e. Silica sand S8 and samples SAM3 and SAM6 had more coarse particles i.e. silica sand S4—hereafter referred to as GI and GIII samples, respectively. Similarly, sample SAM 4 had the same content of silica sand S4 and S8—hereafter referred to as GII samples. The grain sizes of samples are presented in Fig. 3.3. Based on these samples, experiments were conducted for failed and not failed dam conditions.

Again, from laboratory practice, three mixtures of artificial silica sand were selected for the experiments to study the relationship of seepage water volume and TSS of landslide dam failure. Different proportions of a combination of silica sands S4, S5, S6, and S8 were used here in after called Group B sample (Table 3.2). The main part of the sample was silica sands S5 and S6. Silica sands S4 and S8 were considered as coarser and finer particles, respectively, and mixed with silica sands S5 and S6. Three samples, i.e., S456, S4568, and S568, respectively, were prepared in the presence and absence of silica sands S4 and S8. The grain size distributions of the samples are shown in Fig. 3.4.

Table 3.1 Silica sand and kaolinite mixed ratio of samples (Group A sample)

Sample number	SS 4 (kg)	SS 5 (kg)	SS 6 (kg)	SS 8 (kg)	Kaolinite (kg)	Water (kg)	Total (kg)	D_{50} (mm)	C_u	C_c
SAM 1	0.5	4.5	5.0	0.5	0.5	0.5	11.5	0.275	2.456	.980
SAM 2	0.5	4.5	5.0	1.0	-	0.5	11.5	0.290	2.723	1.035
SAM 3	1.0	4	5.5	0.5	-	0.5	11.5	0.375	3.631	0.945
SAM 4	0.5	4.5	5.5	0.5	-	0.5	11.5	0.383	2.659	1.281
SAM 5	-	5.0	5.0	1.0	-	0.5	11.5	0.805	2.856	0.984
SAM 6	1.0	5.0	5.0	-	-	0.5	11.5	0.198	1.914	0.974

D_{50} = median grain size; C_u = coefficient of uniformity; C_c = coefficient of curvature

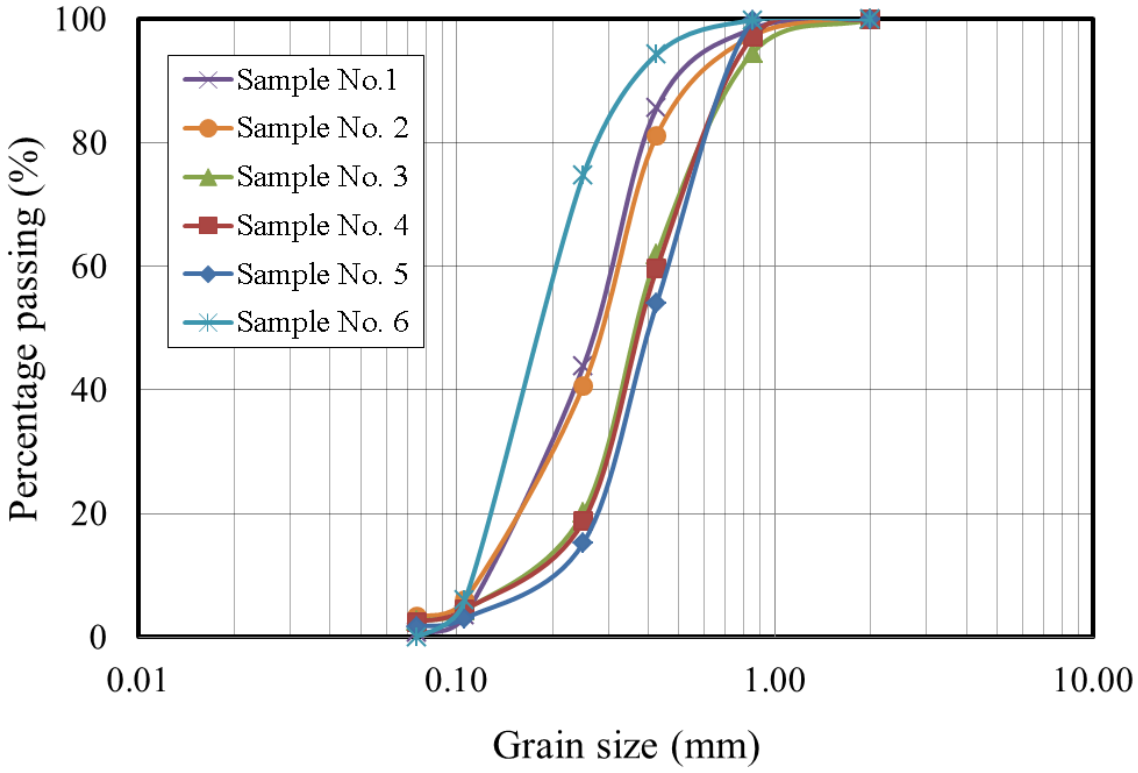

Fig. 3.3 Grain size distribution curves of samples used in experiments (Group A sample)

Table 3.2 Mixed ratios and mechanical properties of samples (Group B sample)

Sample number	SS 4 (kg)	SS 5 (kg)	SS 6 (kg)	SS 8 (kg)	Water (kg)	Total (kg)	D_{50} (mm)	C_u	C_c
S456	1	5	5	-	0.5	11.5	0.394	3.075	1.375
S4568	0.5	4.5	5.0	0.5	0.5	11.5	0.565	2.185	1.098
S568	-	4	5.5	1	0.5	11.5	0.557	2.264	1.065

D_{50} = median grain size; C_u = coefficient of uniformity; C_c = coefficient of curvature

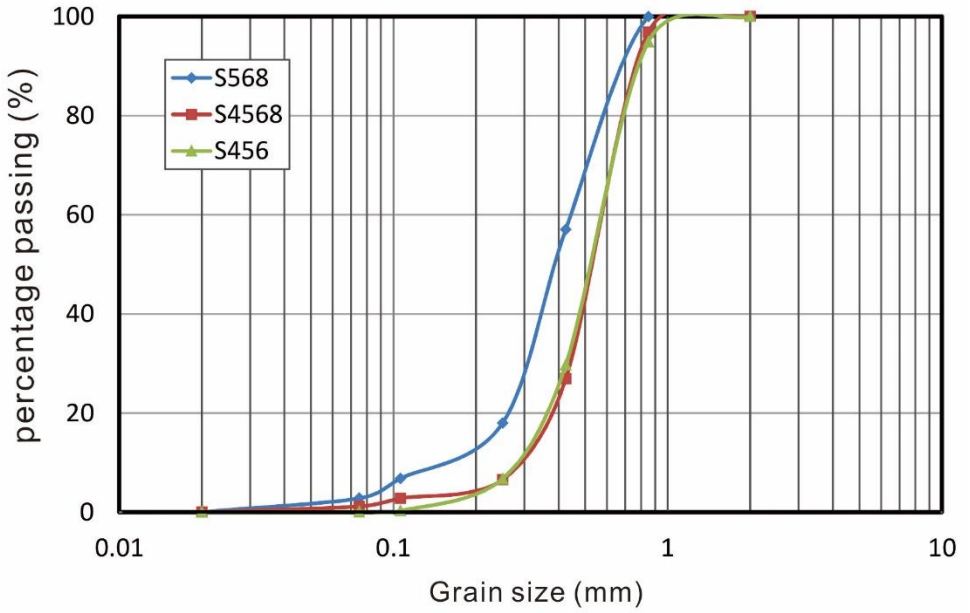

Fig. 3.4 Grain size distribution curves of samples used in experiments (Group B sample)

3.3 Method

A mixing machine was used for mixing the dam materials. Initially, the materials were weighed and poured into a mixing machine with water and mixed for five minutes for Group A samples. For Group B sample, the mixing machine was used for dry mixing, followed by mixing with water for affording the desired shape of the dam. Before creating the dam in the flume tank, a sample was collected to estimate its initial water content. In addition, sensors were placed in their respective positions, and the dam was prepared by layer-to-layer compaction, divided into four and six parts for dam heights of 0.2 m and 0.25 m, respectively. Each layer comprised ~9 kg of sample, and 1–2 kg of sample was used to obtain the final shape of the dam. Real-time data were collected using universal recorders (KYOWA PCD 330B and PCD 400). Sampling frequency was two of data per second. A stopwatch was used during the collection of a seepage water sample for TSS. Seepage water was collected using a half-cut PVC pipe under the flume

tank, facing upwards. Each sample was collected for about 10 sec (± 2 sec). After collecting a sample for TSS, volume was measured and oven-dried using 105ºC temperatures. The dried sample weight was measured, and the TSS value was calculated. Seepage water was directly collected into a tank using the half-cut PVC pipe, and Pwp4 was used to measure the volume for sample group II. The hydraulic gradient was calculated using the pressure head of two sensors, i.e., Pwp1 and Pwp2, respectively, and the flume tank slope (Eq. 2.1). Pwp1 and Pwp2 were fixed below the dam crest edge downstream and upstream of the dam, respectively. Table 3.3 shows the group of samples for failure and not failure case of Group A sample.

Table 3.3 Sample groups based on percentage of fine and coarser particles and, failure condition (Group A sample)

Description	Group I (GI)	Group II (GII)	Group III (GIII)
Failure	SAM 5, SAM 2	SAM 4	SAM 3, SAM 6
Not failure	SAM 1	SAM 4	SAM 3, SAM 6

CHAPTER 4

The relationship among the premonitory factors of landslide dam failure caused by seepage: An experimental study

4.1 Introduction

Landslides or rock avalanches can form landslide dams if their moving mass is sufficient to change the hydrological dynamics of a river channel and form a reservoir (Costa and Schuster 1988; Canuti et al. 1988; Ermini and Casagli 2003; Kourp et al. 2010; Tacconi et al. 2018). The life span of these natural dams depends upon different natural factors. The failure of these dams creates additional and catastrophic disasters. According to the history of landslide dam failure, about 34% of landslide dams have failed within a day of their formation. Similarly, 87% of all landslide dams fail within a year of their formation (Fig. 4.1). These statistics also indicate that about 40% of landslide dams have a medium life span. These dams should be investigated after within a short period of their formation for a risk reduction plan to be made for saving the life and property located downstream of it. A better understanding of premonitory factors, which can easily be measured or observed in actual landslide dams that are at high risk of failure, is important for disaster reduction (Wang et al. 2018). A landslide dam that has not failed for more than one year could allow enough time for investigation, resulting in a high accuracy of prediction in comparison to those landslides that have a life span between two days and several months. In this scenario, those landslide dams with a short life span are very

important for the study of the premonitory factors, especially to discover in which conditions they would fail. These studies would directly support the engineers and decision-makers of disaster management teams of the life and property safety at the downstream site.

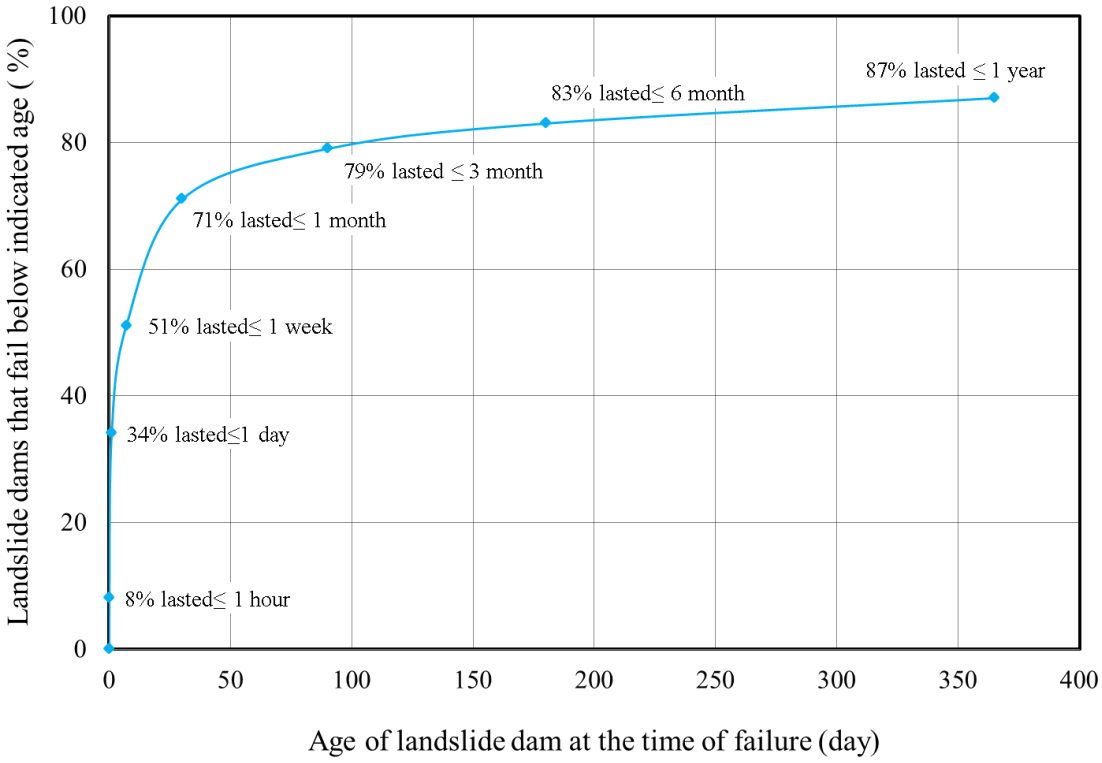

Fig. 4.1 Age of landslide dam at the time of failure (240 cases) (Peng et al. 2012)

It has been shown that the failure of a dam can be divided into the four periods: 1) the emerging of seepage water and front wetting, 2) the hyper-concentrated flow discharge, 3) the emergence and development of a dam crest and 4) the failure of a dam crest with a sharp increase in its subsidence (Wang et al. 2018). The additional question is: What will be the conditions for the failure or stability of a landslide dam?

The inflow rate rate into the reservoir as well as the magnitude, dam size and dam material are relevant for the failure of a landslide dam (Schuster and Costa 1986). An approach utilizing the Dimensionless Blockage Index (DBI) has previously been proposed for the stability analysis of landslide dams, as shown below (Eq. 4.1):

$$DBI = Log(A_b * \frac{H_d}{V_d}) \quad (4.1)$$

where Ab is the area of a basin or reservoir, Hd is the dam height and Vd is the volume of the dam material. DBI is directly related to the geometry of a dam structure and reservoir size. Statistical analysis has indicated that a dam is stable when DBI is < 2.75, quasi-stable when it is $2.75 < \text{DBI} < 3.08$ and unstable when DBI is > 3.08 (Ermini and Casagli 2003). However, some records did not satisfy this equation. Some of them, having large DBI values showing their instability, have existed for a very long time and vice-versa (Storm 2013).

The hydraulic gradient is defined as a head loss, with respect to the distance travelled by a flow of water through a media, as seen in Eq. 4.2:

$$i = -\Delta h/L \quad (4.2)$$

where i = the hydraulic gradient, Δh = the head loss and L = the distance travelled by water. Similarly, the flow of seepage volume can be calculated as seen in Eq. 4.3:

$$Q = kiA \quad (4.3)$$

where Q is the seepage discharge, k is the hydraulic conductivity, i is the hydraulic gradient and A is the area through which the discharge flows. In a laboratory, utilizing a pore water sensor, the total head in the defined positions can be measured. Using the formula of pore water pressure ($u = \gamma wh$), the total head can be calculated considering the dam and flume tank geometry. Seepage water is a very important factor for a landslide dam, which is visible on its downstream side at the actual landslide dam field. The parameters related to seepage water can enlighten the failure process of a landslide dam. Darcy (1856, cited in Fredlund et al. 2012) and Okeke and Wang (2016a) have noted that the seepage flow velocity into a dam is directly dependent upon the hydraulic gradient, as shown in Eq. 4.4:

$$v_w = k_w \frac{dh_w}{dz} \tag{4.4}$$

where Vw = the flow rate of water (m/s), kw is the permeability coefficient with respect to the water phase (m/s) and dhw/dz = the hydraulic gradient in the z-direction. Due to the pressure difference between the upward slope and the downward slope of a landslide dam, the seepage flow occurs in those dams that produce a seepage force. At the time of seepage flow, when the seepage force becomes greater than the erosion resistance force, soil particles begin to move with the seepage water.

Internal erosion is a major cause of embankment dam failure (Fell et al. 2003). Internal erosion that is caused by flow along pre-existing openings, such as cracks in cohesive material or voids along with a contact between the soil-structures (Richards and Reddy 2007), has a higher possibility of occurrence in landslide dams because of their formation process. Erosion as the cause of landslide dam failure has previously been addressed by researchers (Wang et al. 2018;

Okeke and Wang 2016b; Richards and Reddy 2007). Unfortunately, this potential failure mode cannot be completely analysed using numerical formulae or models. Seepage monitoring and analysis for landslide dams may be one premonitory factor in the field. According to Cedergren (1977), seepage failures have two types: (1) failure caused by erosion of soil particles and (2) failure caused by saturation and seepage forces. Jones (1981) has suggested that piping processes involve the dispersion of clay. The Dispersion Index method has been developed by Richie (1963) to determine the dispersity of soil. Richie (1963) has defined 33% of the soil fractions, with less than 0.004 mm dispersing after being shaken in water for 10 min, as indicative of potential failure by tunnelling for earth dams in Australia. Thus, fine particles are responsible for piping failure.

Rather than being initiated by a Darcian flow at an exit point, internal erosion is initiated by the erosive force of water along a pre-existing planar opening (Richards and Reddy 2007). When pore water pressure increases on the downstream side of the dam, the competent cohesion of the soil would decrease. Reduction in cohesion reduces the resistance force and increases the seepage force that can erode the soil particles, as described by Eq. 4.5:

$$F_s = \gamma_w i \tag{4.5}$$

where Fs = the seepage force per unit volume, i = the hydraulic gradient and γw = the unit weight of water. Detailed research on seepage erosion for slope failures has been conducted by Rinaldi and Casagli (1999), Lobkovsky et al. (2004), Wilson et al. (2007), Fox et al. (2007) and many more.

In situ, the turbidity of downstream water provides the rate of erosion from the dam material, which plays a direct role in the subsidence and stability of a dam in the presence of a seepage water flow. According to Wang et al. (2018), the monitory factors remain unchanged at the initial stage as well as in the second stage; the turbidity and vertical displacement starts to slightly increase. Total suspended soils (TSS) also support to understand the erosion into the dam material. Turbidity and TSS are identical premonitory factors that can be measured in both the field and laboratory settings. Fine particles, which are in between the coarser grains, are almost free from effective overburden and capable to migrate by a very low-velocity seepage flow (Takaji and Yusuke 2008). Such eroded particles can be measured as TSS.

By causing light to be scattered, the concentration of suspended particles may have a meaningful correlation to turbidity. Although a variety of parameters, such as density, size and shape of particles as well as water colour, may affect the relationship between the values of TSS and turbidity (Nasrabadi et al. 2016). The correlations between TSS and turbidity have been discussed in detail in a wide range of case studies. A common linear relationship may be defined as shown in Eq. 4.6:

$$TSS = m * Turbidity\,\{NTU\} \tag{4.6}$$

Rügner et al. (2013) have found linear relationships between TSS and turbidity with m values of 1–2.8 $\mathrm{mg\,l^{-1}\ NTU^{-1}}$ (average 1.9 $\mathrm{mg\,l^{-1}\ NTU^{-1}}$) for naturally suspended sediments in rivers in southern Germany. Other studies report slightly lower or higher m values (e.g., 1.1 $\mathrm{mg\,l^{-1}\ NTU^{-1}}$ for particles from karstic springs or up to 3 $\mathrm{mg\,l^{-1}\ NTU^{-1}}$ for suspended sediments in the Lake Tahoe basin, respectively) (Schwarz et al. 2011; Stubblefield et al. 2007).

In the laboratory, the flume tank can be designed to collect seepage water for conducting TSS test. Sample collection time can be simulated to the time of computer using different methods and can relate to other monitoring factors.

Remote sensing is an important monitoring tool in the sphere of natural disaster research these days. Using geographic information system (GIS) and interferometric synthetic aperture (InSAR) technology, the displacement of dams can be monitored regularly. Commercial and non-commercial satellite images are available from different agencies. Images from both before and after an event can be analysed to monitor the landslide dam. Studies, based on GIS and remote sensing, provide useful results for management and engineers. The subsidence of landslide dam crest can be monitored in situ using simple technology for example laser levelling machine can be used. Since subsidence can be monitored, the relation of vertical displacement to other monitoring factors would be very useful to predict the failure of landslide dam.

However, studies have been conducted on different type of landslide dam failure likely overtopping, piping and seepage. Most of these studies have highlighted failure patterns and some studies have focused on seepage failure and internal erosion like Fell et al. 2003; Okeke and Wang 2016a. Conducting an actual comparative study for understanding the stable condition and failure conditions of landslide dam is still necessary. The effect of erosion on TSS and its relation to other premonitory factors of landslide dam has not been well thought out yet.

Hence, this this research aimed to establish the relationship between the premonitory factors of landslide dams during the failure process. Here, the hydraulic gradient was measured using pore water pressure sensors and the vertical displacement was measured using a laser sensor at the dam crest and from the seepage water collected from the dam site to measure its TSS. The intention was to relate the TSS to the hydraulic gradient and the vertical displacement during the

failure process using a combination of different grade of artificial sand particles. The main aim of this study was to identify the real conditions for failure that can be measured or understood in the field. Only seepage failure was considered.

4.2 Results and Discussion

In this work, experiments are conducted to test the failure and stable conditions of a dam crest. Table 3 shows the experiment numbers and their statuses (either failed or stable). Experiments are conducted with GIII, GII, and GI samples to compare the failed and not failed conditions with respect to the hydraulic gradient, vertical displacement, and TSS. The inflow rate into the reservoir is the key to obtaining the failed and not failed conditions. The inflow rate in this study can be understood from the reservoir level, i.e. pore water pressure at Pwp3. Stability and time of failure of dam crest decreases with increase in inflow rate into the reservoir (Okeke and Wang, 2016a). Similarly decrease in inflow rate will increase the stability and failure time. However, experiments of GI samples EXP5FR1, EXP5FR2, EXP5FR3 are failed in all attempts, in spite of low inflow rates than in the GII sample of not failed condition. Thus, it can be concluded that fine samples can fail easily. Additional figures in the annex cover additional experiments with GIII and GI samples of failure and not failure cases.

Table 4.1 Initial state of samples and result of experiment (Group A sample)

Experiment no.	Sample no	Initial Moisture content (%)	Dry density (kg/m^3)	Result of experiment
EXP 2F1	SAM 2	4.3	1529	Failure
EXP 3F	SAM 3	4.5	1227	
EXP 4F	SAM 4	4.3	1272	
EXP 5FR1	SAM 5	4.4	1479	
EXP 5FR2		4.7	1479	
EXP 5FR3		4.3	1526	
EXP 6F	SAM 6	4.3	1287	
EXP 3NF	SAM 3	3.9	1247	Not failure
EXP 4NF	SAM 4	4.4	1262	
EXP 6NF	SAM 6	4.3	1299	
EXP 1NF	SAM 1	4.4	1294	

The reservoir was connected by a pipeline to the main water supply in the laboratory room. When the reservoir started to fill up, Pwp3 sensor started to respond. Seepage began instantaneously and, as the water level in the reservoir increased, the water pressure also began to increase in the dam body and Pwp2 started to respond. Pwp1 sensors also responded after some time. Due to pressure head differences between Pwp1 and Pwp2, the hydraulic gradient began to increase and reached the peak value. Seepage of water continued to flow downwards and the pore water pressure at Pwp1 started to increase and the hydraulic gradient started to

decrease. Using the formula for pore water pressure ($u = \gamma wh$), the water height has been calculated and, using Eq. 4.2, the hydraulic gradient is calculated by considering the slope angle of the flume tank. The rapidly increasing water content in the dam material supports the seepage water flow out of the dam. If the upward seepage forces on a body of soil exceed the gravitational forces at the point of exit, the vertical critical gradient will exceeded and soil particles may be removed from this area (Terzaghi et al. 1996). When the reservoir starts to fill up, the seepage force will increase and will exceed the gravitational forces and seepage water starts to come out with soil particles. The collected seepage water sample was oven-dried to measure the TSS. The dam and reservoir size, the slope of the flume tank, the position of sensors and the seepage water collection position was fixed for all experiments.

4.2.1 Characteristics of the premonitory factor for failure cases

4.2.1.1 Results of GI sample

Experiment No. EXP 2F was conducted for the GI sample. The reservoir began to fill up, with an increase in pore water pressure in Pwp3, resulting in the wetting of dam material front. The initial moisture content of the sample was 4.3% only. The saturation level has been increasing continuously, and the colours of the dam material also change from light to dark. The water level has increased at the Pwp2 sensor after about 600 s of Pwp3. The difference between the two-pore pressure inside the dam—i.e., Pwp2 and Pwp1—was high. The hydraulic conductivity of the soil would be affected by the particle size; the finer particles have low permeability. The experimental results are presented in Fig. 4.2. The hydraulic gradient was increased rapidly as pore water pressure increased in Pwp2 and reached the peak value, highest within this study. The hydraulic gradient began to decrease from the peak value as Pwp1 started to increase. The

vertical displacement began to increase slowly at a nearly constant rate and then it rapidly increased prior to the dam crest failure. Wang et al. (2018), Okeke and Wang 2016a are also presented same pattern of hydraulic gradient for the real sample of landslide dam failure and for silica sand respectively. The downstream slope was continuously changing its topography due to the increase in water content and seepage failure. The vertical displacement was about 2.5 mm just prior to the failure of the dam crest. The hydraulic gradient began to decrease from its peak value and the seepage water started to come out on the dam's downstream side. An initial value of TSS was quite a bit higher in most experiments. TSS initially decreased and then began to increase slowly. Wang et al. (2018) also present that the turbidity of downstream seepage water has increased before the failure. The vertical displacement rate was very low before the seepage water came out and, after the seepage water flow, the rate of vertical displacement increased. The hydraulic gradient slowly started to increase as the downward slope failure increased and, at the same time, the reservoir level also increased—finally, the dam crest failed.

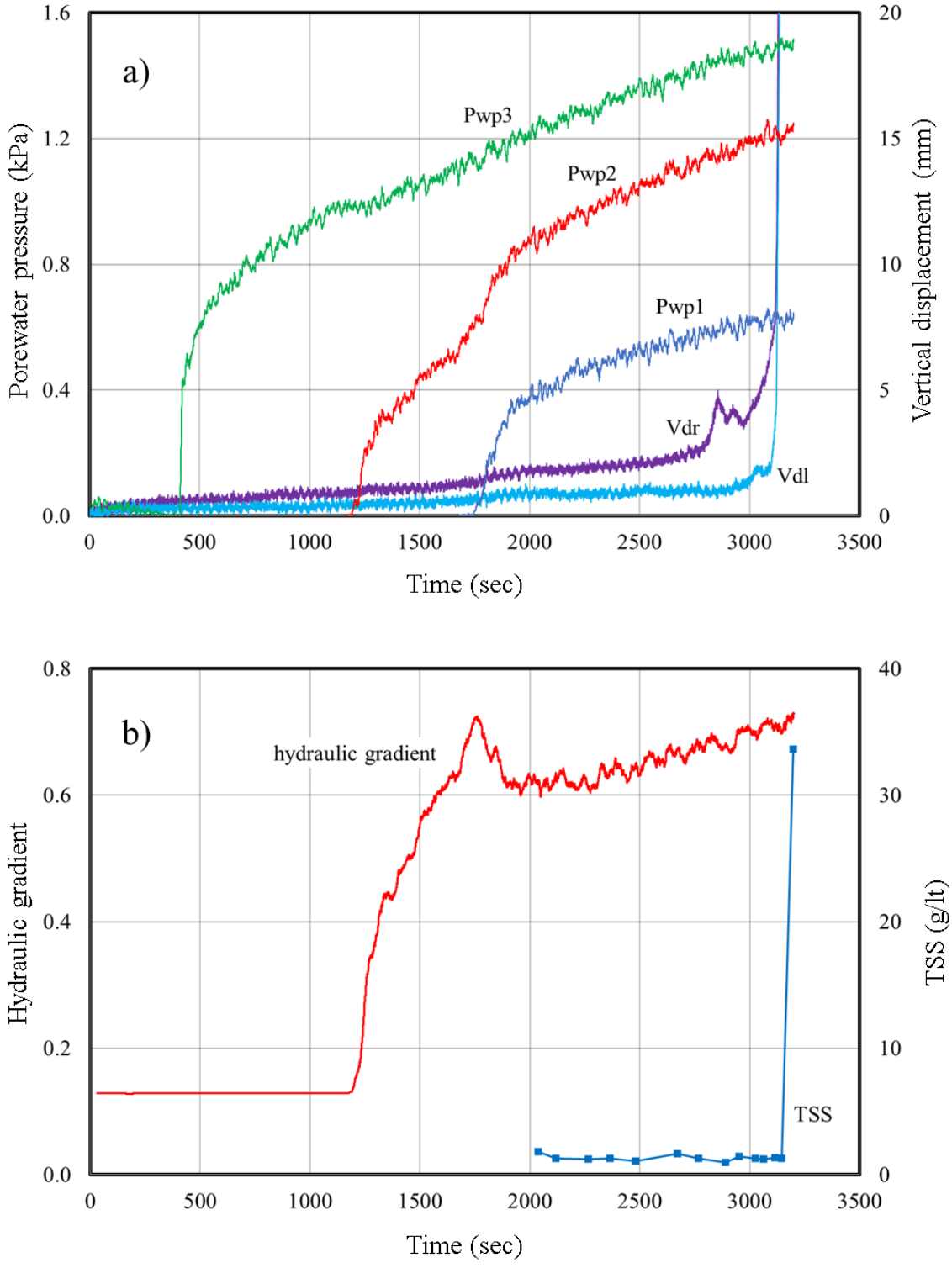

Fig. 4.2 Experiment results of experiment No. EXP 2F of GI sample. a) Pore water pressure and vertical displacement; b) Hydraulic gradient and TSS

4.2.1.2 Results of GII sample

Experiment No. EXP 4F was conducted for the GII sample. The wetting front was rapidly increased just after the beginning of the reservoir fill up. The pore water pressure was increased at Pwp3 as the reservoir started filling up and Pwp2 also began to increase after Pwp3 started. Pwp1 began at nearly the same time as Pwp2. The pore water pressure at Pwp2 is increased very quickly and, as a result, the hydraulic gradient also increased very quickly, from about 0.2 to 0.6. Due to a sudden failure of a small soil mass block from the upper part of the slope of the dam's downstream side, the seepage water flow is stopped and the water pressure at Pwp1 is increased, which also affected the hydraulic gradient. Figure 4.3 shows the details of the experiment results. Initially, the hydraulic gradient reached the peak value but it does not decrease again to the minimum value, unlike in the other experiments in this study, and again started to increase instead. The hydraulic gradient was unsteady. Reasons for the fluctuation of the hydraulic gradient are: 1) the release of water from the downstream into different pocket areas of the downstream slope and 2) the failure of the downward slope and the decreased position of the flow line. The vertical displacement was nearly constant at the initial stage and, as the hydraulic gradient is increased, the vertical displacement also increased. Due to the appearance and disappearance of minor cracks in the dam crest, the vertical displacement is increased and later decreased. The vertical displacement is about 0.85 mm prior to the failure of the dam crest. Figure 4b shows that seepage began when the hydraulic gradient reached the initial peak value. Considering the time gap, due to the position of the seepage collection point, the vertical displacement began to increase when TSS is measured. With the changes in the hydraulic gradient and the increasing TSS, the dam became unstable and, finally, failed.

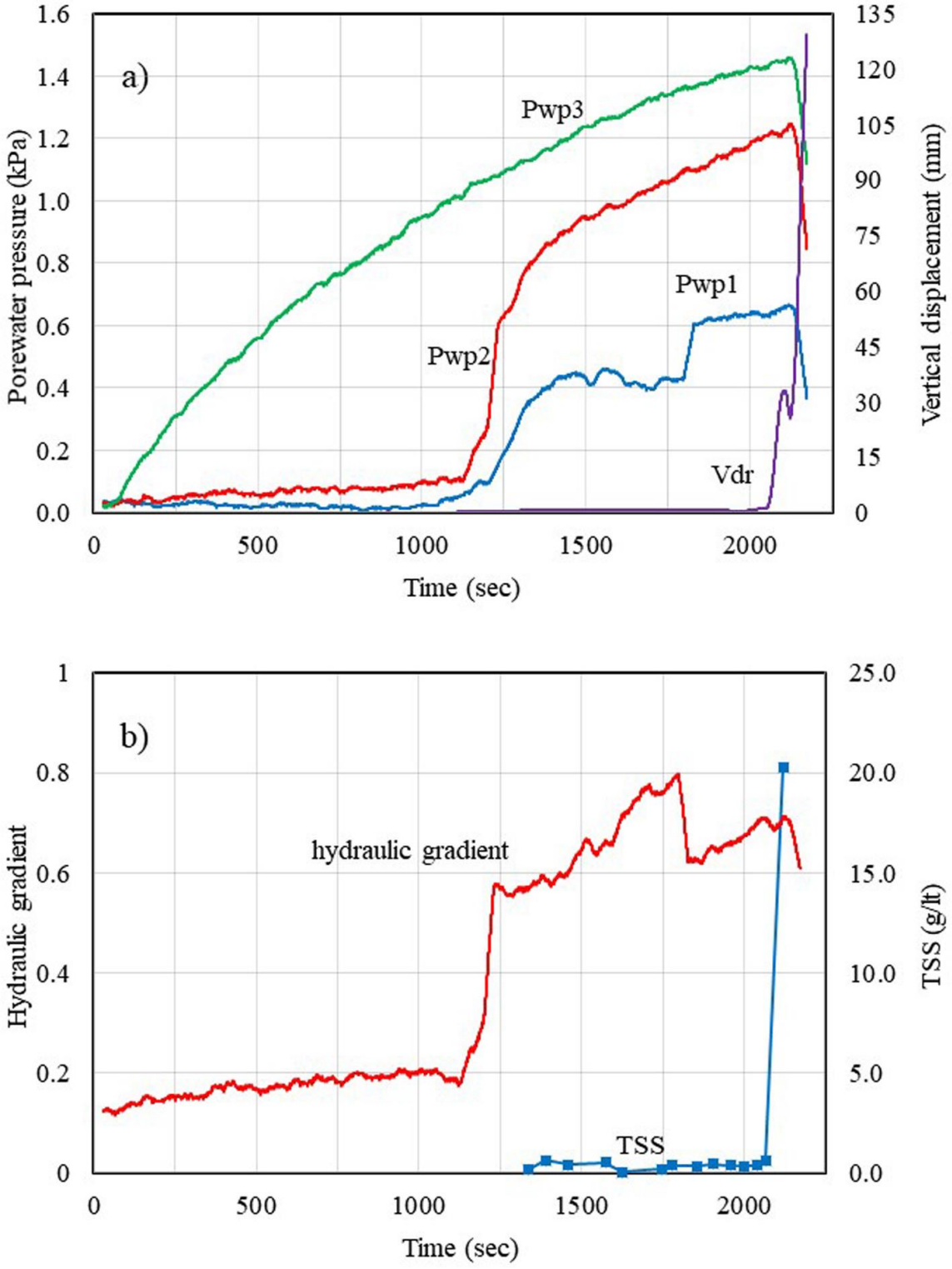

Fig. 4.3 Experiment results of experiment No. EXP 4F of GII sample. a) Pore water pressure and vertical displacement; b) Hydraulic gradient and TSS

4.2.1.3 Results of GIII sample

Experiment No. EXP 6F was conducted for the GIII sample. Here, the seepage water has a great effect on the erosion and stability of the dam body. The coarser soil had a higher hydraulic conductivity and a higher chance of erosion of the fine particles. The pore water pressures at Pwp2 and Pwp1 began to increase very quickly in comparison to the GI and GII samples. The pore water pressure at Pwp2 increased rather quickly and, after approximately 250 s, the pore pressure at Pwp2 and Pwp1 become equal. The water level increased in the downstream side of the dam, as a result of which the slope failed. As the slope failed, the position of the flow line changed and the pore pressure at Pwp1 increased with its decreasing rate. The results are presented in Fig. 4.4. The vertical displacement started to increase as the hydraulic gradient increased. This could be the effect of changes in the water content of the dam body. The up and down movement of the vertical displacement is the result of the sudden presence and absence of minor cracks at the dam crest. The hydraulic gradient reached the peak value and started to decrease as the pore pressure increased in Pwp1. After reaching the low value of the hydraulic gradient, it slowly increased as the water level increased in the reservoir and slope edge failed of the downstream slope. The hydraulic gradient changed with the change in the topography of the downward slope. As the pore water pressure reached approximately 1.4 kPa at Pwp3, the vertical displacement increased rapidly and the dam crest failed. The seepage water began to come out at about 500 s of the peak hydraulic gradient. The GIII sample has big voids, due to which the fine soil particles, which were in-between the coarse particles, came out with the seepage water—resulting in higher turbidity. The TSS value is approximately 1.2 g/lt, which was higher in comparison to that of the GII and GI samples without kaolinite.

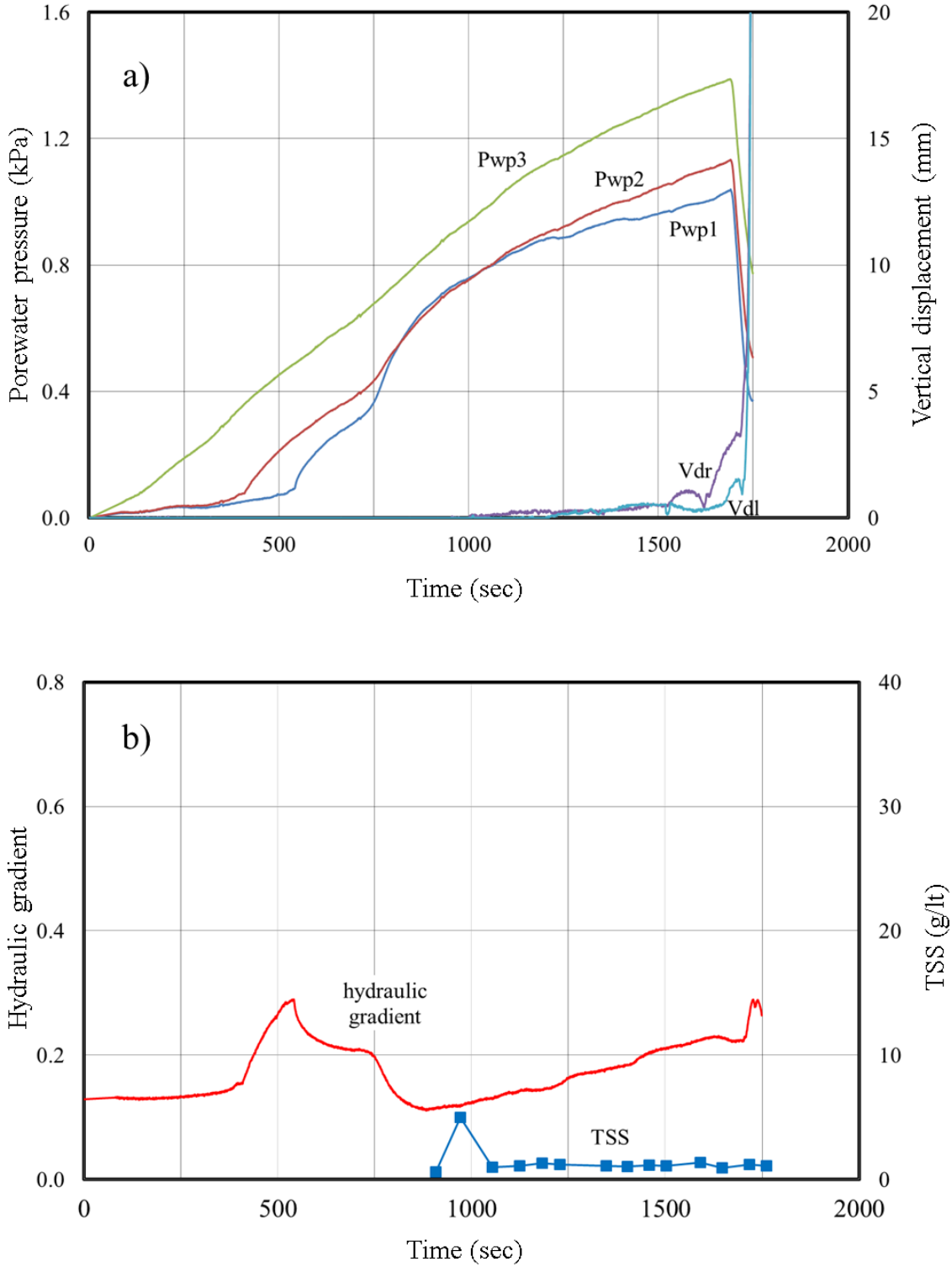

Fig. 4.4 Experiment results of experiment No. EXP 6F of GIII sample. a) Pore water pressure and vertical displacement; b) Hydraulic gradient and TSS

4.2.2 Characteristics of premonitory factors for the non-failure cases

4.2.2.1 Results of GI sample

Experiment No. EXP 1NF was conducted on the GI sample with kaolinite. Kaolinite is only used in this experiment to understand the effect of minerals on premonitory factors. The pore water pressure at Pwp2 began to respond 500 s after it began to respond at Pwp3. The pore water pressure at Pwp2 increased more quickly and became nearly equal to that of Pwp3. Similarly, Pwp1 also increased about 250 s after Pwp2 started. Figure 4.5 shows the experiment results. The hydraulic process of this experiment is nearly the same as in the other experiments in which kaolinite is not used. The vertical displacement increased as the hydraulic gradient started to decrease from the peak value. This experiment is continued for about 7000 s and it is stopped and defined as a non-failure case when the pore water pressure at Pwp1, Pwp2 and Pwp3 became nearly constant. The vertical displacement and hydraulic gradient became constant as Pwp2 and Pwp1 become nearly constant. The maximum hydraulic gradient is about 0.47 and the vertical displacement is less than 1 mm during the experiment.

The seepage velocity inside the landslide dam would be very low and distant travel by the seepage water would not occur in a straight line. Thus, the eroded particles would travel in different directions and, finally, come out with the seepage water. If there are more fine particles, the seepage water would erode more particles with a low velocity. Here, in this experiment, due to the presence of kaolinite, the TSS value is very high in contrast to that of other experiments. The seepage water came out from the dam after the hydraulic gradient decreased to its minimum value from its peak value. Similarly, displacement has been noticed as the seepage water began to come out. Fine samples without kaolinite are also has the same nature of curves of the hydraulic gradient, TSS, and the vertical displacement but the value of TSS is significantly low

in these experiments. Here, the constant hydraulic gradient and decreasing TSS are the causes of the dam crest not-failure.

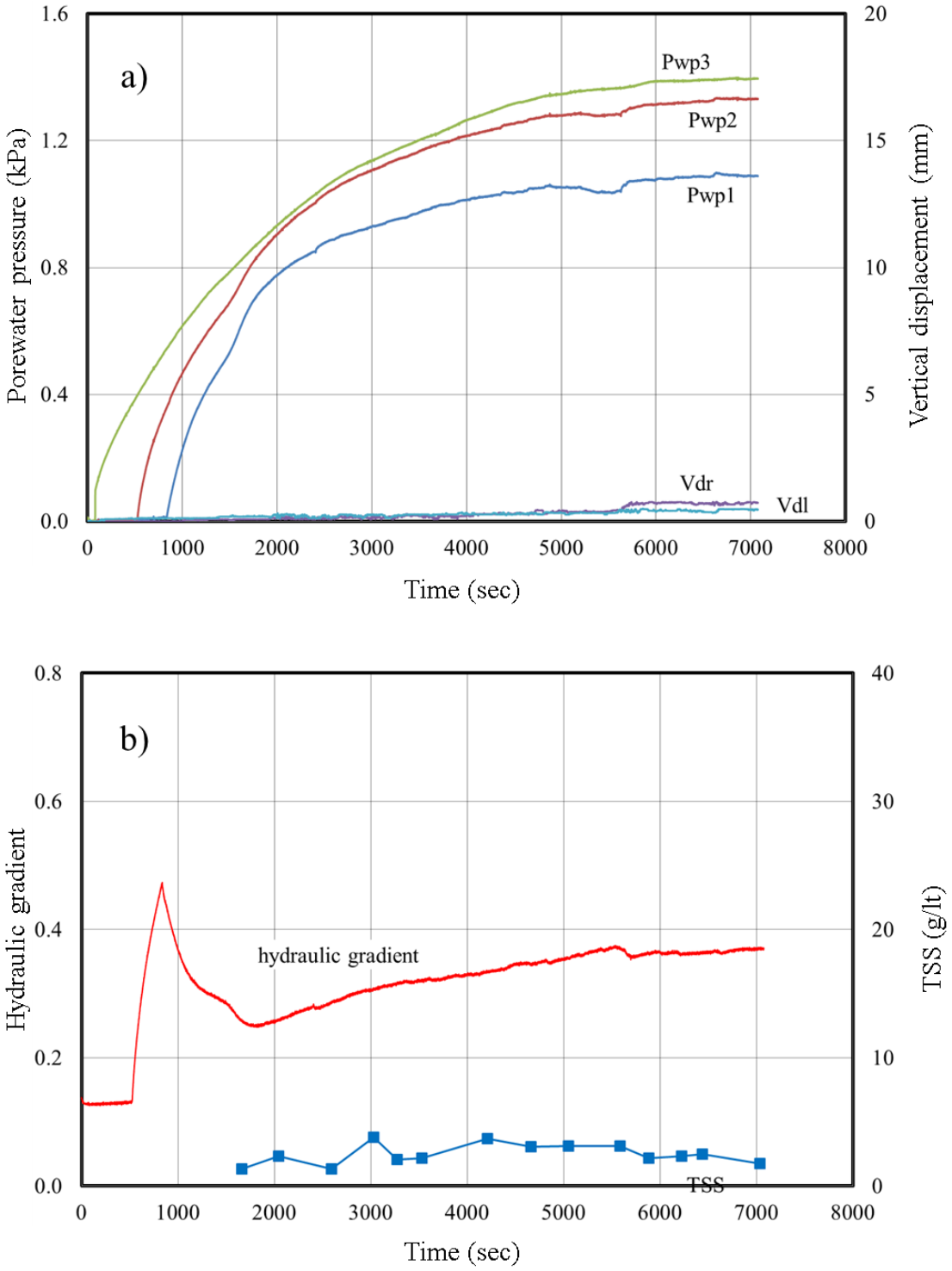

Fig. 4.5 Experiment results of experiment No. EXP 1NF of GI sample (with kaolinite). a) Pore water pressure and vertical displacement; b) Hydraulic gradient and TSS

4.2.2.2 Result of GII Sample

Experiment No. EXP 4NF was conducted for the non-failure case of the GII sample. As in the failure case (EXP 4F), initially, the pore water pressure increased at Pwp2 and Pwp1 together. The hydraulic gradient reached the peak value and started to decrease and the vertical displacement is constant at about 0.5 mm during the experiment; however, at last, it reached 2.5 mm due to a small crack formation. The downstream slope topography was continuously changing due to the increase in the water level and seepage failure. After approximately 4000 s, the pore water pressure at Pwp3 became nearly constant. Figure 4.6 shows the results of the experiment. This condition can be considered as the inflow rate into the reservoir and the seepage water rate from the dam body is the same. At the same time, the pore water pressure at Pwp2 is also constant, which additionally proved that the dam is stable. Although the maximum value of the hydraulic gradient is about 1.2 at 3000 s, the dam crest is stable, which shows the importance of the vertical displacement and the seepage water TSS for failure. The seepage water began to come out after the hydraulic gradient decreased to the minimum value from its peak value. The hydraulic gradient reached the maximum value and started to decrease, while the TSS value also decreased. During the experiment, it is visualized that the turbidity of the water decreased. Finally, the TSS became zero. The vertical displacement is nearly constant throughout the experiment, at less than 0.5 mm. The changes in the water content in the dam material and at the dam crest surface could have an effect on the vertical displacement, which can be noticed in this experiment. Here, the constant vertical displacement and the decreasing TSS are the main causes of the dam crest non-failure.

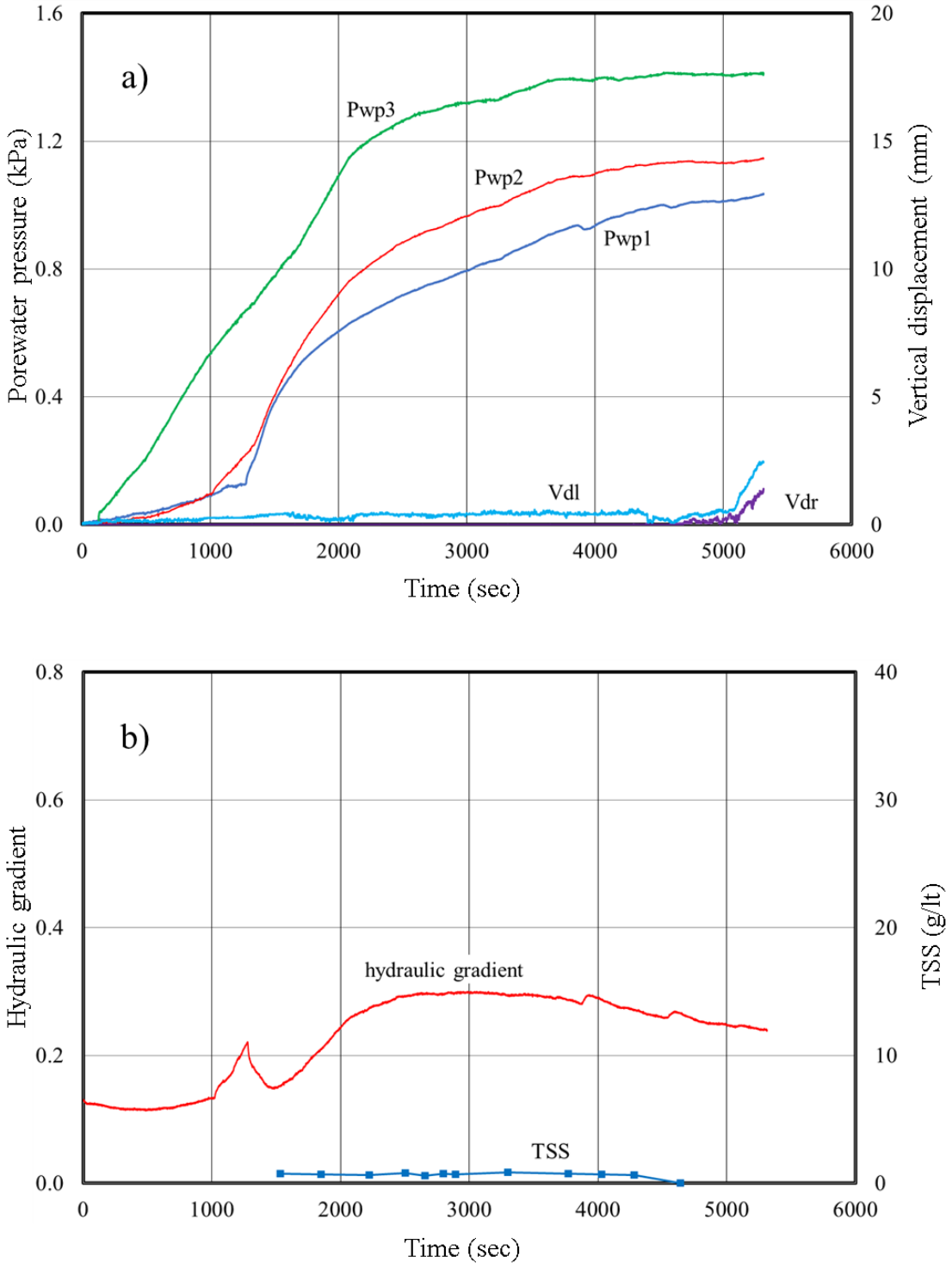

Fig. 4.6 Experiment results for experiment No. EXP 4NF of GII sample. a) Pore water pressure and vertical displacement; b) Hydraulic gradient and TSS

4.2.2.3 Result of GIII Sample

Experiment no. EXP 3NF was conducted for the non-failure case of the GIII sample. The hydraulic gradient result obtained in this experiment is typical in this study, where the hydraulic gradient reached the peak value and become constant. The pore water pressure at Pwp2 and Pwp1 increased at the same time as in the failure case experiment. The rate of increase for Pwp2 and Pwp1 differed from that in the failure case for the same sample. The vertical displacement increased from when the hydraulic gradient began to increase—i.e. when the water level started to increase in the dam body. The vertical displacement increased very slowly, up to about 3.0 and 4.0 for Vdl and Vdr, respectively. Finally, the vertical displacement became constant and the pore water pressure in the reservoir started to decrease, which may be due to the higher rate of seepage water than of inflow into the reservoir. Figure 4.7 shows the experiment results. The maximum hydraulic gradient of this experiment is approximately 0.67, which is higher than in the failure case for a coarse sample. The seepage water came out after 1850 s—i.e. just after the hydraulic gradient reached the peak value. The vertical displacement increased simultaneously with seepage water. After reaching 1.5 mm, the vertical displacement increased rapidly until 3.7 mm and became constant. This experiment shows that the presence of TSS and the increment of the vertical displacement are not the only satisfactory conditions for failure but that the role of the hydraulic gradient also needs to be considered. The hydraulic gradient should reach the peak value, then decrease to the minimum value and once again start to increase as in the failure case presented in this report. In this experiment, the hydraulic gradient is the main cause behind the dam crest not-failure.

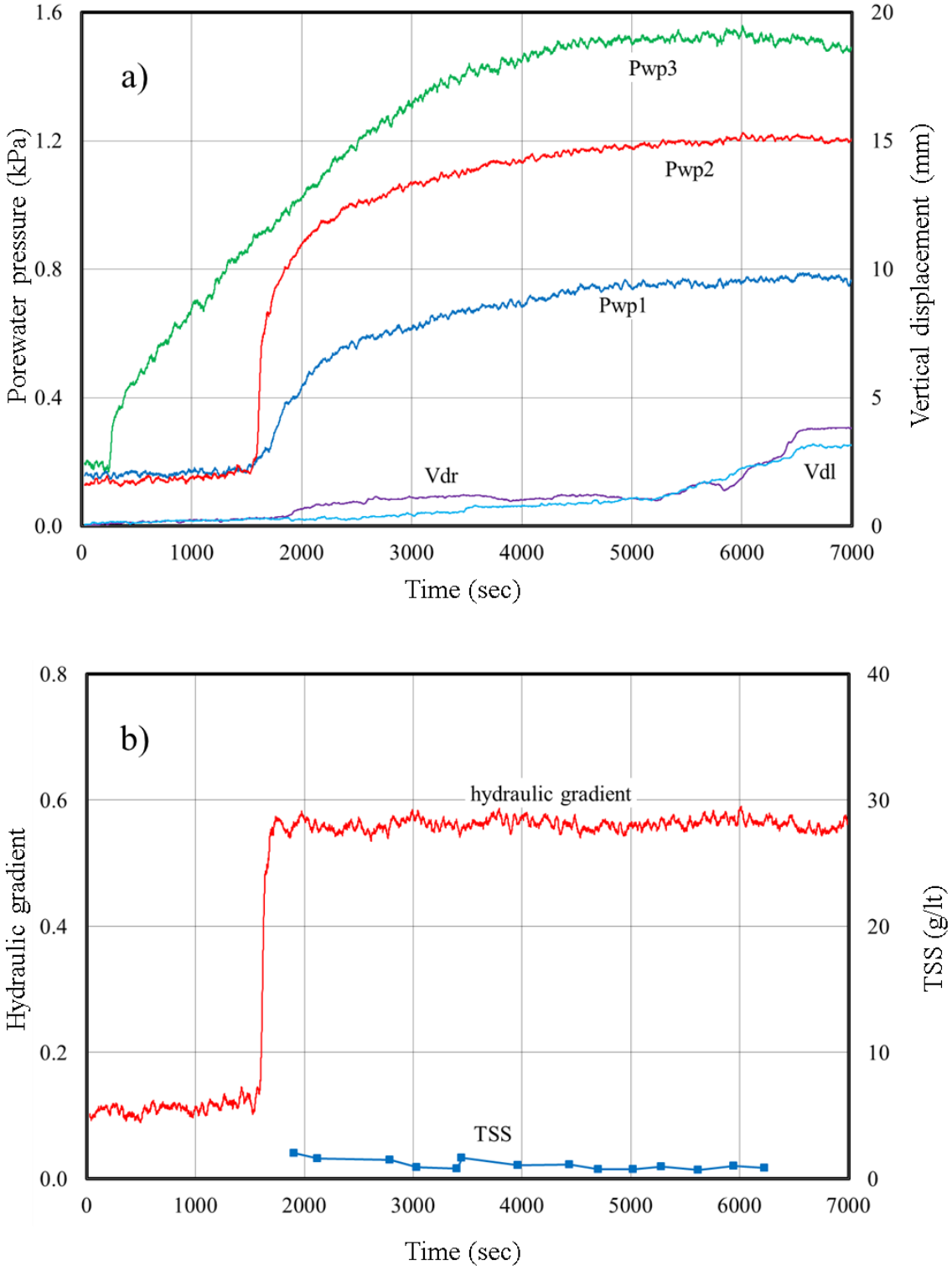

Fig. 4.7 Experiment results of experiment No. EXP 3NF of GIII sample. a) Pore water pressure and vertical displacement; b) Hydraulic gradient and TSS

4.2. 3 Characteristics of TSS for the failure and non-failure cases

Figures 4.8 and 4.9 show the TSS characteristics during both the failure and non-failure cases, respectively. These TSS graphs are conscripted after the removal of the initial and final data for the failure cases and the initial data for the non-failure cases. Except for sample no. 3, for the failure case, all experiments show that TSS increased before the failure of dam crest. The TSS trend lines for the different experiments are presented in Figs. 4.8 and Fig. 4.9 with equations. From the Fig. 4.8, it can be understood that the nature of TSS in failure cases increased before the failure but the rate of TSS increment is diverse in different samples. The TSS is high for sample GII, medium for sample GIII and lowers for sample GI. Fine particles, which are in between the coarser grains, are almost free from effective overburden and capable to migrate by a very low-velocity of seepage flow (Takaji and Yusuke 2008). As sample GII has both the silica sand S4 and S8 in equal percentage, the TSS is measured higher. An interesting characteristic is noticed for non-failure—that the slope angle of trend line of TSS is nearly same for the GI, GII and GIII samples. It can be concluded that, if the TSS trend line slope is larger and decreasing, then it could be predicted that a landslide dam would not fail. The velocity of seepage water depends upon the hydraulic gradient. The seepage velocity plays a role in the erosion of soil particles. In this report, when comparing the results of the experiments performed, it is found that the higher the value of the hydraulic gradient, higher the TSS value also. The TSS value is higher for the GII and GIII samples than for the GI sample; however, the fine sample with kaolinite has the highest TSS value.

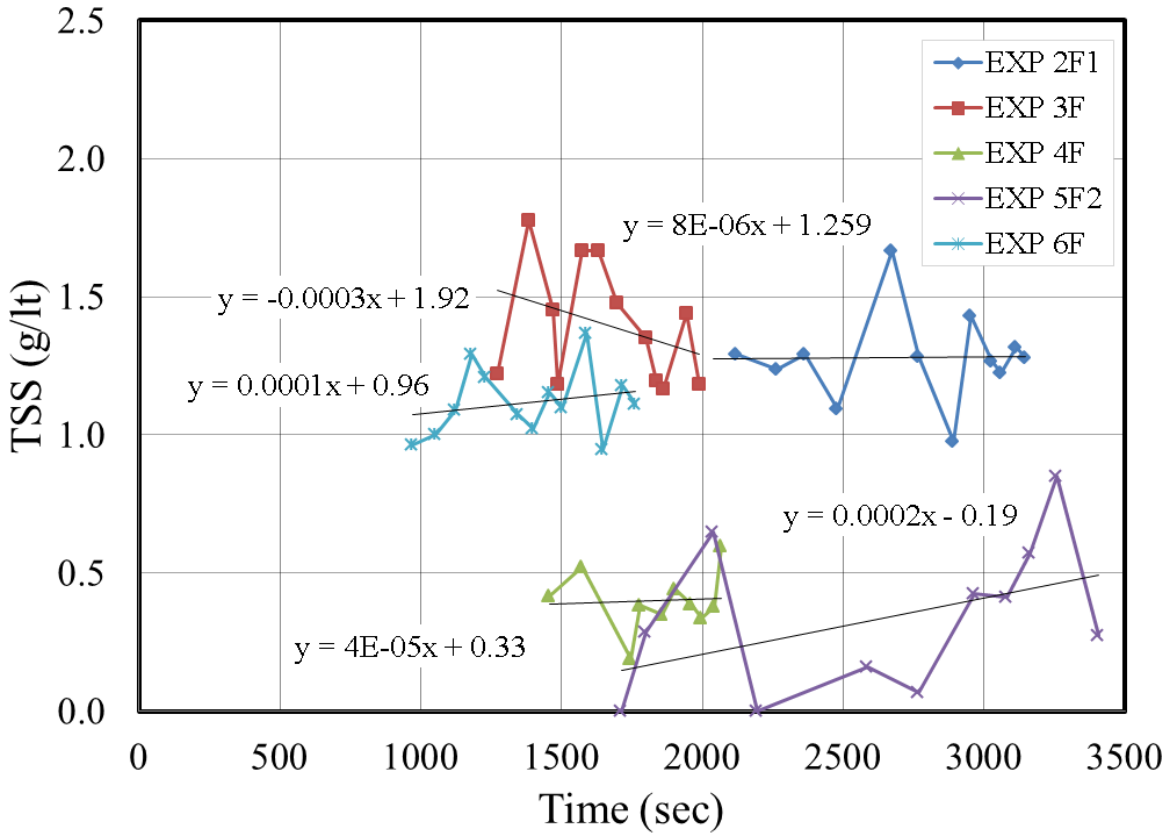

Fig. 4.8 TSS trend for different samples (failure condition)

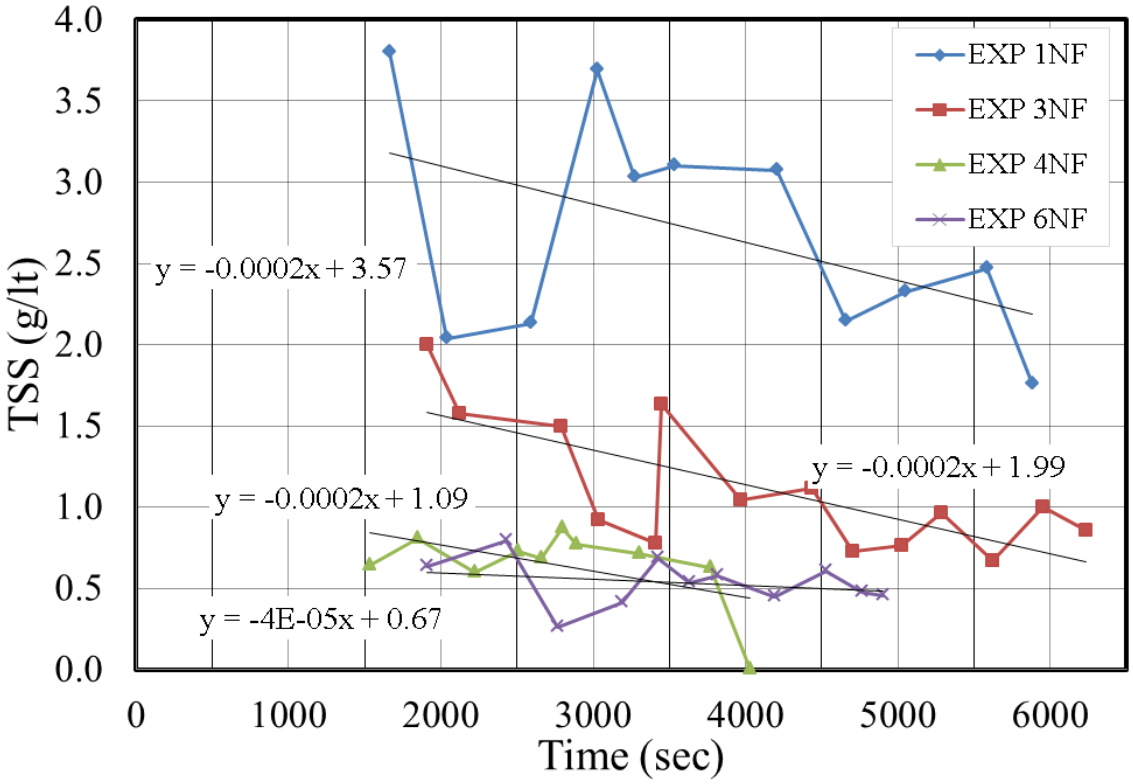

Fig. 4.9 TSS trend for different samples (non-failure condition)

CHAPTER 5

Relationship between seepage water and total suspended solids of landslide dam failure caused by seepage: An experimental investigation

5.1 Introduction

Formation and failure of landslide dams in mountainous areas constitute a significant natural hazard. A majority of landslides that block rivers are either caused by heavy rainfall or earthquakes (Schuster and Costa, 1986; Canuti et al., 1988; Costa and Schuster, 1988; Korup, 2004; Evans et al., 2011; Peng and Zhang, 2012; Casagli et al., 2003; Tacconi at al., 2018). As the landslide mass shifts from its original position to the river, it may contain debris and loose soils. Hence, a landslide dam is composed of heterogeneous or poorly consolidated material with debris. A landslide dam differs from a constructed embankment dam as it exhibits no control structure for seepage and drainage (Uhlir, 1998; Awal et al., 2007). A better understanding of premonitory factors, which can easily be measured or observed in actual landslide dams that are at high risk of failure, is crucial for disaster reduction (Wang et al., 2018). In real fields, due to the high risk of failure, limited parameters such as seepage quantity, turbidity of downstream seepage, vertical displacement of the dam crest, reservoir level, and impounded area can be monitored (Dhungana and Wang, 2019).

The inflow rate into the reservoir and reservoir volume, dam size, and dam material are important factor that affect the failure of a landslide dam (Schuster and Costa, 1988). Some

authors already reported the statistics of landslide dams and their failure in various regions worldwide. They have summarized the important characteristics of landslide dams including their classification, cause and type of failure, life span, and some other important parameters (Costa and Schuster, 1991; Korup, 2004; Stefanelli et al., 2015; Xu et al., 2009; Casagli and Ermini, 1999; Chai, 1995; Clague, 1994).

Overtopping, piping, and seepage failure constitute the typical failures of landslide dams. Dams comprising homogeneous soil mostly undergo failure by seepage and downstream slope saturation (Dunning et al., 2006), whereas piping holes are formed in dams that are built with mixed soil, depending on the percentage of the fine content and the interlocking bond between soil particles.

Failure sequence of a dam was reportedly categorized into four periods: 1) emergence of seepage water and front wetting, 2) hyper-concentrated flow discharge, 3) emergence and development of a dam crest, and 4) failure of a dam crest with a sharp increase in its subsidence (Wang et al., 2018). Dhungana and Wang (2019) described the conditions for the failure and stability of the landslide dam for seepage failure, where trends of total suspended solids (TSS) and the hydraulic gradient were compared under failure and stable conditions.

Internal instability is a failure mode of soil subjected to seepage. The seepage failure mode is characterized by the erosion of fine particles through the pore matrix of the coarse fraction of the soil (Richards and Reddy, 2007). Due to the erosion of fine particles, the flow path undergoes expansion, leading to the resistance strength loss of the external load (Ahlinhan et al., 2016).

In addition, TSS supports the understanding of the dam material erosion. Turbidity and TSS are identical premonitory factors that can be measured under field and laboratory settings (Rugner et al., 2013; Stubblefield et al., 2007). Fine particles, which are among coarser grains, are almost

free from effective overburden and it can migrate under an extremely-low-velocity seepage flow (Takaji et al., 2008). Such eroded particles can be measured as TSS in the laboratory and in the field (Dhungana and Wang, 2019).

Several studies (Rinaldi and Casagli, 1999; Lobkovsky et al., 2004; Wilson et al., 2007; Fox et al., 2007) reported detailed research on seepage erosion for slope failures. Numerous experimental methods were used to simulate the development of internal erosion in earth dams and landslide dams (Wit et al., 1981; Brauns, 1985; Maknoon and Mahdi, 2010; Wang et al., 2018; Okeke et al., 2016a, 2016b). Hanson et al. (2010) analyzed the variation in the erodibility of different soil materials due to the internal erosion of dams by large-scale outdoor model tests. They observed that the rate of erosion in different soil materials varies in order of magnitude.

Chang et al. (2011) conducted field erodibility tests on two landslide dams triggered by the 12 May 2008, Ms 8.0 Wenchuan earthquake in the Sichuan Province of China and revealed that an increase in the bulk density is inversely proportional to the coefficient of erodibility with depth. Furthermore, Hanson et al. (2010) conducted large-scale physical tests to investigate the impact of erosion resistance on internal erosion in embankment dams and revealed that erosion resistance for the same embankment material increases with the increase in the compactive effort and water content.

Many studies have been conducted on different landslide dam failures, possibly overtopping, piping, and seepage (Awal et al., 2007, 2011; Wang et al., 2018). A majority of these studies highlighted failure patterns, but only a few studies focused on the seepage failure and internal erosion. In addition, effects on the turbidity, seepage volume, and failure mechanism with different parameters of landslide dams were not examined.

Hence, this study aimed to highlight the relationship between the seepage volume and TSS of landslide dams during failure. In this case, the hydraulic gradient was measured using pore-water pressure sensors; vertical displacement was measured using a laser sensor at the dam crest; seepage water was collected, and seepage volume was monitored using a pore-water pressure sensor. A seepage water sample was collected, and TSS was measured.

5.2 Results and Discussion

5.2.1 General characteristics of the experiments

Dam failure leads to flash floods on the downstream side. Hence, it is crucial to understand the failure pattern of landslide dams to minimize natural hazards caused by floods. In this study, experiments were conducted to understand the effect of the dam height, reservoir size, and inflow rate into the reservoir on hydraulic gradient, vertical displacement, TSS, seepage water volume, and longevity of the dam for three soil samples prepared by the mix of silica sands S4, S5, S6, and S8. Table 2 summarizes the experimental details.

Table 2 Outline of all experiments under different testing conditions (Group B sample)

Exp. No	Sample type	Inflow rate (m^3/s)	Dam height (m)	Reservoir size	Dry density (kg/m^3)	Initial moisture content (%)
Exp1	S568	$1.1*10^{-5}$	0.2		1294	2.7
Exp2		$1.67*10^{-5}$			1251	2.7
Exp3			0.25	R1	1269	2.8
Exp4				R2	1223	3.2
Exp5	S4568	$1.1*10^{-5}$	0.2		1334	2.7
Exp6		$1.67*10^{-5}$			1301	2.9
Exp7			0.25	R1	1234	2.8
Exp8				R2	1241	2.7
Exp9	S456	$1.1*10^{-5}$	0.2			
Exp10		$1.67*10^{-5}$			1302	2.5
Exp11			0.25	R1	1275	2.8
Exp12				R2	1202	3.0

Time of landslide dam failure is key factor to reducing natural disasters. In this study as well, dams failed at varying periods under different conditions. The time factor plays roles in soil saturation and shear strength reduction. From experiments, the higher the percentage of silica sand S8 in the dam material, the shorter the life span of the dam. Higher the percentage of silica sand S4 in the dam material, the longer the life span of the dam. Despite this observation, a longer time was taken for the seepage water to drain out from the dam body for a sample containing silica sand S8. The density of the dam controlled the time for the initial peak

hydraulic gradient, whereas density exhibited a lower effect for the total life span in contrast to the initial peak hydraulic gradient (Fig 5.1).

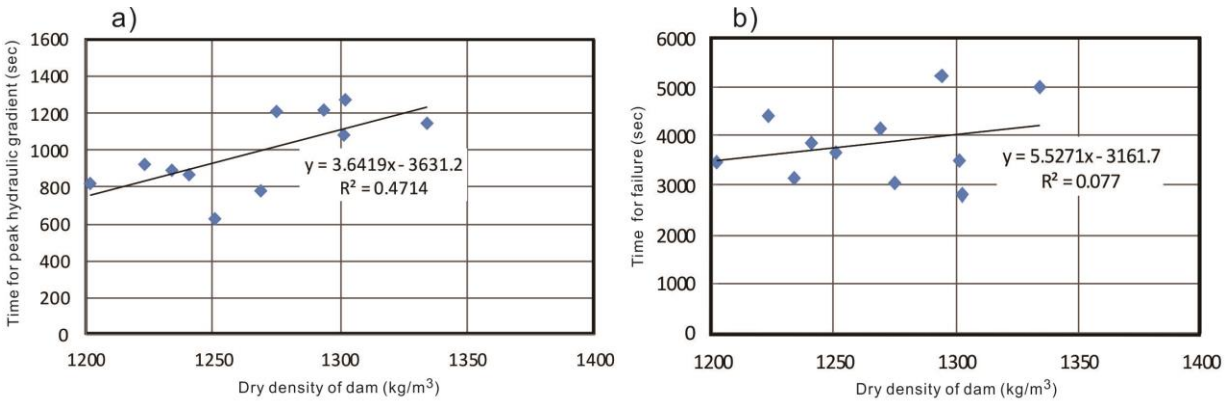

Fig. 5.1 Effects of density on a) time for initial peak hydraulic gradient and b) time for failure of dam crest

5.2.2 Effect of inflow rate on dam failure

Experiments were conducted with three samples, i.e., S456, S4568, and S568, respectively, for inflow rates of 1.1×10^{-5} m^3/s and 1.667×10^{-5} m^3/s. Inflow rate were selected based on the practice on these samples to get the seepage failure. Experimental results revealed a time lag between the peak hydraulic gradient (which is responsible for the start of seepage) and seepage flow out time (referred as TSS starting time in figures). Inflow rates into the reservoir created variations in the hydraulic process for different soil types. For the S568 sample, the initial peak hydraulic gradient that started seepage was varied from 0.29 to 0.39 (Fig. 5.2). In case of the higher inflow rate, the hydraulic gradient was decreased from its peak value of 0.39 to 0.23, and again started to increase, and the dam crest underwent failure when it reached 0.28. For the low inflow rate, the hydraulic gradient decreased from its peak value of 0.29 to 0.21 and again started

to increase and undergo failure when it reached 0.39. The rapid increment in the hydraulic gradient initiated the high seepage gradient, leading to the early flow of seepage and shear strength reduction of the dam material. This result in turn led to the high TSS and dam crest settlement. The rapid increase in the hydraulic gradient supported the erosion of soil particles from the dam body, while the seepage volume was comparatively low.

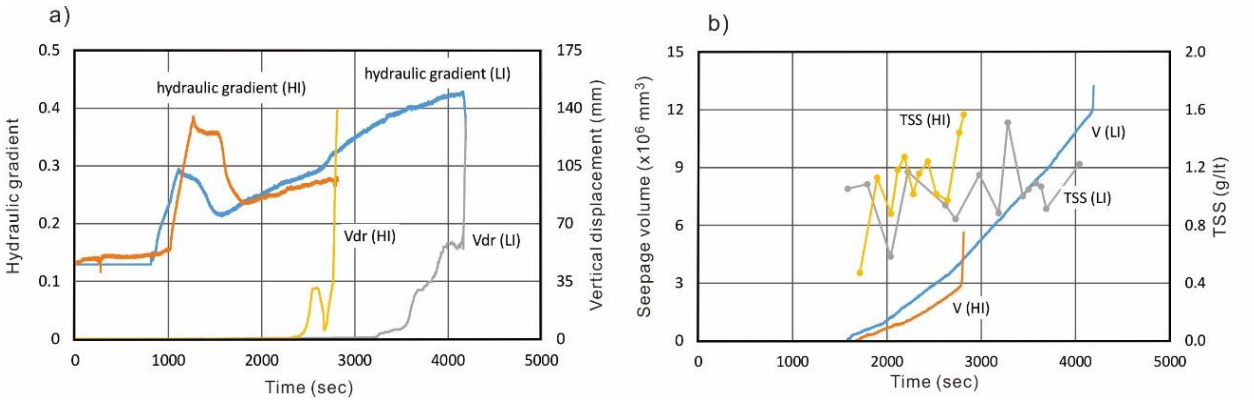

Fig. 5.2 Time series data of hydraulic gradient, vertical displacement, seepage volume and TSS for the sample S568 at a low inflow rate (LI) of 1.1 × 10–5 m3/s and high inflow rate (HI) 1.67 × 10–5 m3/s. a) Hydraulic gradient and vertical displacement; b) Seepage volume and TSS

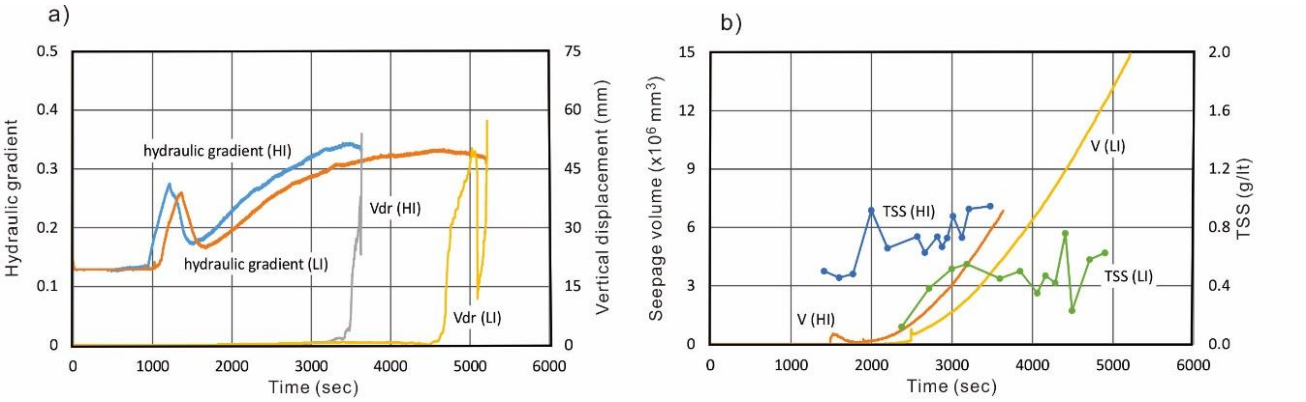

Fig. 5.3 Time series data of hydraulic gradient, vertical displacement, seepage volume and TSS for the sample S4568 at a low inflow rate (LI) of 1.1×10^{-5} m^3/s and high inflow rate (HI) 1.67×10^{-5} m^3/s. a) Hydraulic gradient and vertical displacement; b) Seepage volume and TSS

For the S4568 sample, the initial peak hydraulic gradients were 0.26 and 0.27 for low and high inflow rates, respectively, and at the time of failure, the corresponding values were 0.39 and 0.38 (Fig. 5.3). For the high inflow rate, the total volume of seepage water was lower, and the TSS value was high, related to the higher rate of seepage water released from the dam body. With the increase in the percentage of silica sand S4, the TSS value decreased for both inflow rates; however, the time taken for failure decrease with the increase in the percentage of silica sand S8. For the S456 sample, no failure was observed at an inflow rate of 1.11×10^{-5} m^3/s. The pore water pressure at Pwp2 and Pwp3 became constant after 8000 s, and hence considered as the stable case, whereas for an inflow rate of 1.67×10^{-5} m^3/s, failure was observed within 3700s. The seepage water flow at the lower inflow rate became extremely high, leading to a stable dam crest, whereas the TSS and vertical displacement were constant as reported by Dhungana and Wang (2019). At a high inflow rate, the lowest initial peak hydraulic gradient was observed throughout the study, and the vertical displacement sharply increased before failure. At a low

inflow rate, the vertical displacement increased due to cracks in the dam crest after that horizontal movement occurred and dam crest failed.

5.2.3 Effect of dam height on dam failure

A statistical approach proposed a dimensionless breaking index (DBI) to investigate the stability of the dam (Ermini and Casagli, 2003). This empirical relation predicted the dam stability by using the dam geometry, where the reservoir volumes and dam heights are key parameters. The landslide dam size is the major factor that contributes to the seepage erosion and slope instability. For the soil slope instability, downstream slope angles and the soil layer gradient are major factors that control the critical hydraulic gradient (Iverson and Major, 1986; Budhu and Gobin, 1996). The landslide dam height is a key parameter for examining the stability of the natural dam. The increase in the dam height reduces the stability of the dam crest (Okeke and Wang, 2016b). Experiments were conducted to understand the effect of the dam height on the stability, TSS, and seepage water volume. For the S4568 sample (Fig. 5.4), containing a higher percentage of coarser sand particles and increase in dam height decrease the longevity of dam, which also was in agreement with the results reported by Okeke and Wang (2018), which may be possibly related to the mass block failure in the downstream site and increased percentage of coarser particles and sample S4568 has lowest value of coefficient of uniformity. As the initial peak hydraulic gradient of the higher dam was greater than that of the lower dam, the instability of the internal structure increased, leading to higher TSS on seepage water. The seepage water volume on the downstream side increased with the dam height for all three samples. For the lower dam height, the total seepage volume was limited in comparison to that for the higher dam height within the same period. All three samples in this study revealed that the height between the

reservoir water level and dam crest at the time of failure increases with the dam height; similarly, it increased with the percentage of silica sand S4; however, significant settlement in the dam crest for both cases was observed. The dam crest exhibited cracks during the test for a higher dam, and the crack size increased with the increase in the percentage of silica sand S4.

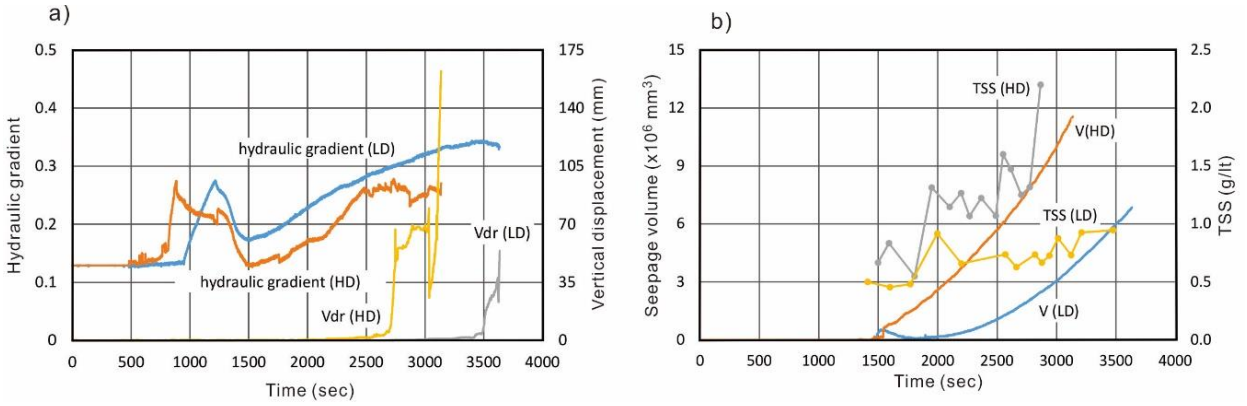

Fig. 5.4 Time series data of hydraulic gradient, vertical displacement, seepage volume and TSS for the sample S4568 at a Low dam height (LD) (200mm) and High dam height (HD) (250 mm). a) Hydraulic gradient and vertical displacement; b) Seepage volume and TSS

5.2.4 Effect of reservoir size on dam failure

Reservoir area is a leading factor in statistical analysis for proposing DBI. The static pressure caused by the river gradient to the dam body increases if the reservoir size increases. The increase in the reservoir level will increase the time for filling up the entire reservoir, which will play a role in the stability of the dam body. The reservoir size was longitudinally increased by 0.1 m, which increased the reservoir area by 0.043 m^2. The total time for the failure of the dam crest increased with the increase in the reservoir size for all three samples. The maximum hydraulic gradient for the experiment with the S456 sample was increased in comparison to those

with the S4568 and S568 samples. Notably, the times for the initial peak hydraulic gradient for the S456, S4568, and S568 samples were nearly the same, whereas for a small reservoir, time for the initial hydraulic gradient increased from S456 to S568.

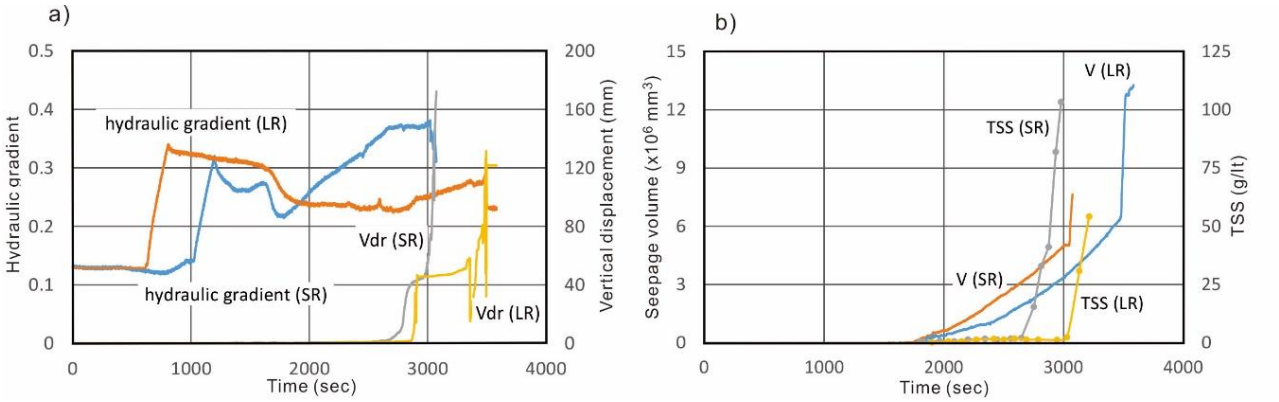

Fig. 5.5 Time series data of hydraulic gradient, vertical displacement, seepage volume and TSS for the sample S568 at a small reservoir (SR) and large reservoir (LR). a) Hydraulic gradient and vertical displacement; b) Seepage volume and TSS

For the S568 sample, for the small reservoir, the hydraulic gradient was greater at the time of failure than the initial peak hydraulic gradient, and for the large reservoir, the initial peak hydraulic gradient was greater than the failure hydraulic gradient (Fig. 5.5). Compared to the small reservoir, a small amount of hydraulic force was observed at the initiation time of internal instability for the large reservoir. The TSS has increased abruptly before the failure of dam crest for both small and large reservoirs. The vertical displacement was high for the large reservoir case, where the seepage water volume was also high, and the failure for half part of the dam crest was noticed for the large reservoir case.

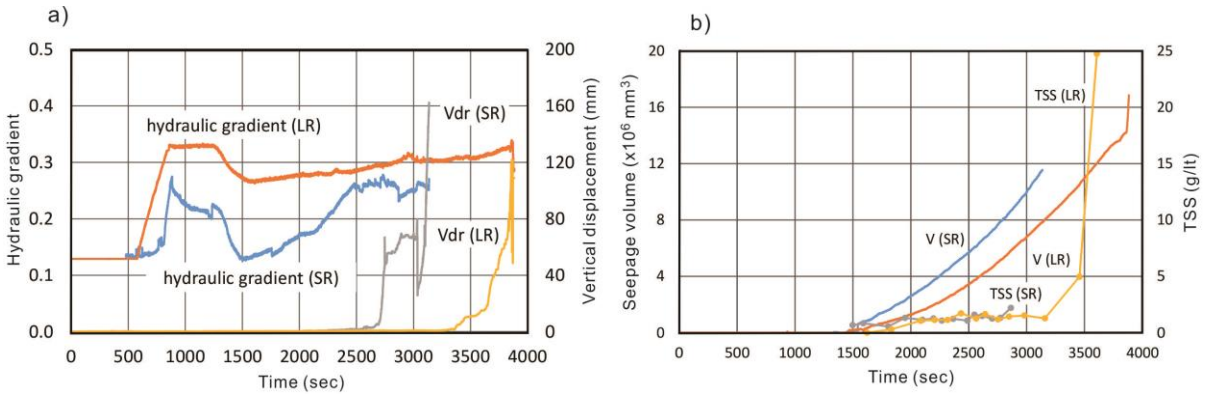

Fig. 5.6 Time series data of hydraulic gradient, vertical displacement, seepage volume and TSS for the sample S4568 at a small reservoir (SR) and large reservoir (LR). a) Hydraulic gradient and vertical displacement; b) Seepage water volume and TSS

For the S4568 sample, the TSS value was greater in case of the small-sized reservoir, due to which the vertical displacement was also high, and the failure of dam crest was observed earlier than in the case of the large-sized reservoir (Fig. 5.6). The initial rate of seepage water volume for the small reservoir was greater, and the cumulative total seepage water volume before the dam failure was greater for the large-sized reservoir. For the small reservoir, due to the higher TSS, internal erosion occurred, and the shear strength of the soil decreased, leading to a low hydraulic gradient at the time of failure compared to that observed for a large-sized reservoir.

For the S456 sample, TSS was nearly constant for the large reservoir and rapidly increased at the time of failure, whereas for the small reservoir, TSS slowly increased with fluctuation (Fig. 5.7). The hydraulic gradient for the small reservoir was less than that for the large reservoir, which was different from other experiments with the S568 sample. Similarly, for the large reservoir, failure hydraulic gradient was highest throughout this study, which may be the effect of the reservoir size. Kokusho and Fujikura (2008) reported that physical parameters such as particle

density, hydraulic conductivity, and gravel content affect the seepage development in landslide dams and soil slopes, which can be used in this experiment. The seepage rate was nearly the same for large- and small-sized reservoirs, but the total seepage volume was greater for the large-sized reservoir. Horizontal displacement was noticed for a small reservoir after the failure of the half part of the dam crest.

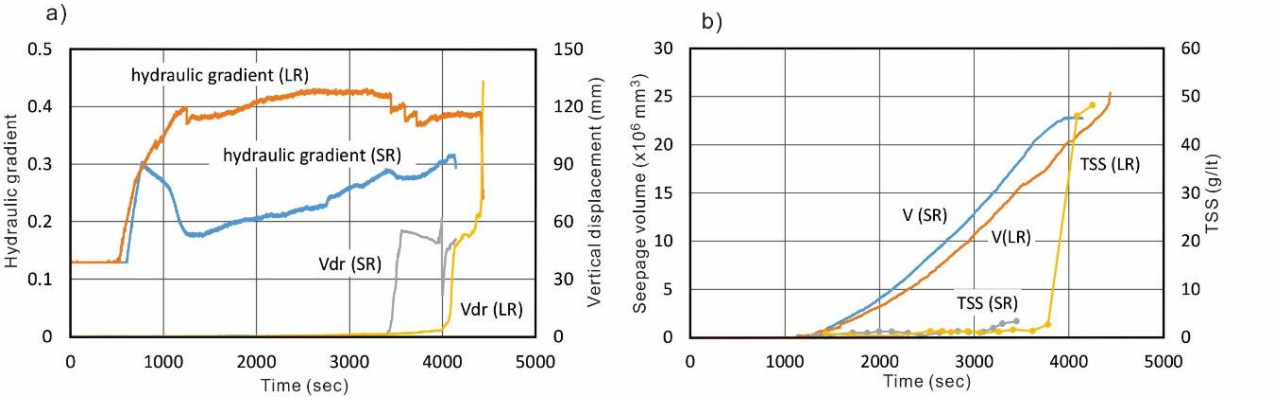

Fig. 5.7 Time series data of hydraulic gradient, vertical displacement, seepage volume and TSS for the sample S456 at a small reservoir (SR) and large reservoir (LR). a) Hydraulic gradient and vertical displacement; b) Seepage volume and TSS

CHAPTER 6

Conclusions

A landslide dam always has the potential for catastrophic failure with high risk for life, and property damage at the downstream site. The formation of a landslide dam is a natural process thus, minimizing the risk due to its failure is important. Landslide dam failure can be categorized into three types: seepage failure, overtopping and slope failure. However, historical statistics of natural dam failures reveal the need for an improved understanding of the complex mechanisms of internal erosion that could aid in the prediction of failure of the dam. As described by other researchers, the established premonitory factors of landslide dam failure are hydraulic gradients, seepage, and turbidity as well as vertical displacement and inflow rate into the reservoir. Knowledge of the internal instability of dam material is the key factor to predict the seepage failure of the landslide dam. Failure time is another factor to reduce the adverse effect of catastrophic floods. The objective of this study is to support field engineers for predicting the failure time of the landslide dam caused by seepage, based on the possible available data in the field without disturbing the dam body. The following are the main conclusion of this study, which supports to predict the failure of the landslide dam.

- The seepage failure of a landslide dam can be predicted by understanding the nature of its premonitory factors. These factors behave differently in different particle size samples.
- The TSS trend line may represent an initial factor to check the stability of a dam crest. A dam crest would fail with increasing TSS and it may be stable with decreasing TSS.

- The sample having a coarser particle would have a higher TSS even with a low hydraulic gradient. The coarser material may get failed with low hydraulic gradient. For samples having more fine particles, the vertical displacement would be very low and it would start to increase just prior to the failure of a dam crest.
- The seepage failure of the downstream side slope would be smooth for samples having higher percentage of fine particles, whereas a mass block failure would occur for samples having higher percentage of medium and coarse particle.
- A dam crest would be stable if its hydraulic gradient becomes constant, which is especially possible for samples having higher percentage of coarse particle.
- Based on all experiments, it can be concluded that the hydraulic gradient has three stages: 1) it begins to increase and reaches peak value, 2) it begins to decrease from the peak value and reaches the minimum value and 3) it begins to increase again when the seepage water starts to come out and the vertical displacement starts to increase.
- Dam failures always occur when the seepage water comes out with an increasing TSS tendency and an increasing vertical displacement while, at the same time, the hydraulic gradient is at its third stage.
- Experiments of the non-failed condition show that there would be either no hydraulic gradient increase, no increment in the vertical displacement or a decreasing TSS or any two of them. In the field, if we could monitor the seepage water and the vertical displacement, it would be easy to predict potential dam failure.
- Experiments conducted on three samples prepared by mixing the silica sand revealed that the time of failure of experiments increases depending on the changes in the percentages of fine and coarser sand. Samples with finer particles exhibited a short dam life span (Fig 6.1).

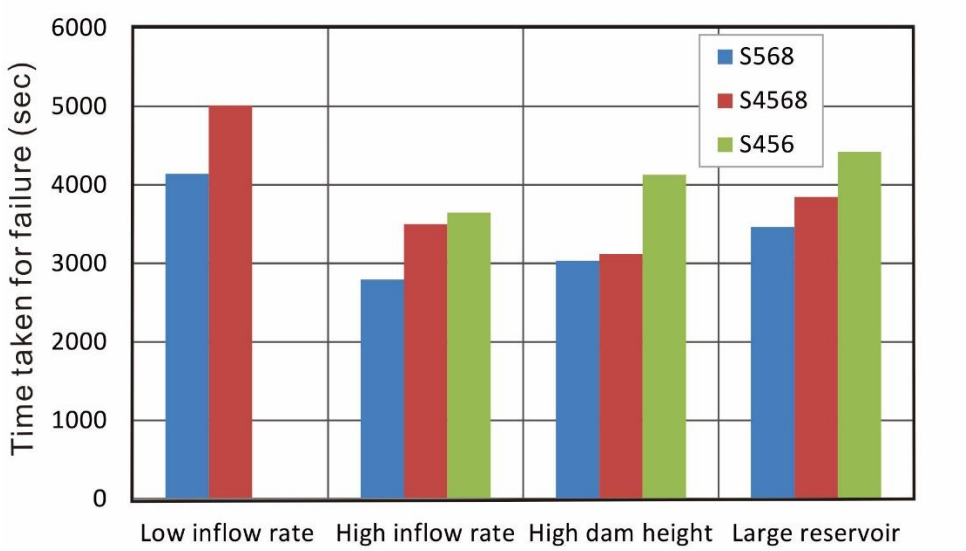

Fig. 6.1 Time taken for failure of dam crest for different conditions

- At a low inflow rate into the reservoir, the hydraulic gradient to initiate the seepage was less than that at the time of failure (Fig. 5.2 and Fig. 5.3). The internal structure was more stable due to the low hydraulic gradient, leading to low TSS and negligible vertical displacement; however, the total seepage volume was high.
- For the sample comprising coarser particles and small coefficient of uniformity may reduce the life span of dam, possibly related to the change in the permeability and effect of the critical hydraulic gradient to initiate the seepage or internal instability.
- With the increase in reservoir volume, the maximum hydraulic gradient exhibited differently as that observed in case of inflow rates and dam height (Fig.6.2), and the seepage water volume increased, and TSS decreased with the increase in the reservoir volume.

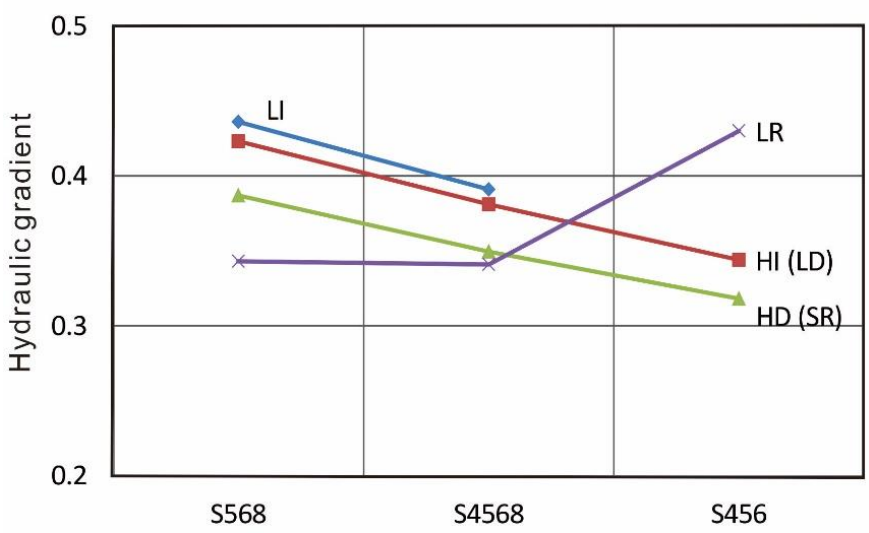

Fig. 6.2 Maximum hydraulic gradient for low inflow rate (LI), high inflow rate (HI), low dam (LD), high dam (HD), small reservoir (SR) and large reservoir (LR) of three samples

- Although there was a continuous process of the hydraulic gradient and seepage and erosion, the hydraulic gradient was predominantly affected by the inflow rate and dam geometry, whereas the total seepage volume, seepage rate, and TSS depended on the particle size of the dam material and reservoir size.

References

Ahlinhan M.F, Koube M.B, Adjovi C.E (2016) Assessment of the internal instability for granular soils subjected to seepage. Journal of Geoscience and Environment Protection, 4, 46-55.

Awal, R, Nakagawa H, Baba Y and Sharma R.H (2007) Numerical and experimental study on landslide dam failure by sliding. Annual Journal of Hydraulic Engineering, JSCE. 51.

Awal, R, Nakagawa H, Fujita H, Kawaike K, Baba Y, and Zhang H (2011) Study on the piping failure of a natural dam. Annuals of Disaster Prevention Research Institute Kyoto University 54: 539–547.

Bo MW, Fabius M, Fabius K (2008) Impact of global warming on stability of natural slopes. In Proceedings of the 4th Canadian Conference on Geohazards: From Causes to Management, Presse de Univ. Laval, Quebec.

Bonnard C (2011) Technical and human aspects of historic rockslide-dammed lakes and landslide dam breaches. In: Evans SG, Hermanns RL, Strom A, Scarascia-Mugnozza G (eds) Natural and artificial rockslide dams. Springer Berlin Heidelberg, pp. 101-122

Brauns, J (1985) Stability of layered granular soil under horizontal groundwater flow. In Proceedings of the 15 th International Congress on Large Dams, vol 1, Lausanne.

Budhu, M, and Gobin R (1996) Slope instability from ground-water seepage. Journal of Hydraulic Engineering 122(7):415–417.

Canuti, P., Casagli N, Ermini L (1988) Inventory of landslide dam in the Northern Apennine as a model for induced flood hazard forecasting. In: Andah K (ed) Managing hydro- geological disaster in a vulnerable environment. Grifo Pub., Perugia, pp 189-202.

Casagli N, Ermini L (1999) Geomorphic analysis of landslide dams in the Northern Apennine. Trans Jpn Geomorphol Union 20(3):219–249.

Casagli, N., L. Ermini, and G. Rosati (2003) Determining grain size distribution of material composing landslide dams in the Northern Apennines: sampling and processing methods. Engineering Geology, 69(1):83-9.

Cedergren, HR (1977) Seepage, drainage, and flow nets. Wiley, New York.

Chai HJ, Liu HC, Zhang ZY (1995) The catalogue of Chinese landslide dam events. Journal of Geological Hazards Environment Preservation; 6(4):1-9.

Chang, D.S., Zhang LM, Xu Y, and Huang R.Q (2011) Field testing of erodibility of two landslide dams triggered by the 12 May Wenchuan earthquake. Landslides 8(3): 321–332.

Chigira M, Yagi H (2006) Geological and geomorphological characteristics of landslides triggered by the 2004 Mid Niigta prefecture earthquake in Japan. Engineering Geology, 82(4):202-221.

Clague JJ, Evans SG (1994) Formation and failure of natural dams in the Canadian Cordillera. Geological Survey of Canada Bullet; 464:1–35.

Costa, JE, Schuster RL (1988) The formation and failure of natural dams. Geol Soc Am Bull 100(7):1054-1068.

Costa, JE, Schuster RL (1991) Documented historical landslide dams from around the world. U.S. Geological Survey; 1991. P.1-486.

Crozier MJ (2010) Deciphering the effect of climate change on landslide activity: A review. Geomorphology, 124(3):260-267.

Dahal R.K and Hasegawa S (2008) Representative rainfall thresholds for landslides in the Nepal Himalaya. Geomorphology, Volume 100 (3–4), 429–443.

Dai FC, Lee CF, Deng JH, Tham LG (2005) The 1786 earthquake-triggered landslide dam and subsequent dam-break flood on the Dadu River, southwestern China. Geomorphology, 65(3):205-221.

DeKay, M. L, and McClelland, G. H (1993). Predicting loss of life in cases of dam failure and flash flood. Risk Analysis, 13(2): 193–205.

Dhital, M. R (2002) Landslide investigation and mitigation in Nepal, Abstracts: 17th Himalaya-Karakorum- Tibet Workshop, India, Journal of Southeast Asian Earth Sciences , Volume 20, Issue 4, Supplement 1, pp 9.

Dhungana P., Wang F (2019) The relationship among the premonitory factors of landslide dam failure caused by seepage: An experimental study. Geoenvironmental Disaster, (Under publication).

Dunning SA, Rosser NJ, Petley DN, Massey CR (2006) Formation and failure of the Tsatichhu landslide dam, Bhutan. Landslides 3:107–113.

Ermini L, Casagli N (2003) Prediction of the behaviour of landslide dams using a geomorphological dimensionless index. Earth Surface Processes and Landforms, 28(1):31-47.

Evans, S.G., K.B. Delaney, R.L. Hermanns, A. Strom, and G. Scarascia-Mugnozza (2011) The formation and behavior of natural and artificial rockslide dams; implications for engineering performance and hazard management. In Natural and artificial rockslide dams, ed. S.G. Evans, R.L. Hermanns, A. Strom, and G. Scarascia-Mugnozza, 1–75. Berlin Heidelberg: Springer.

Fell, R, and Fry, JJ (2007) The state of the art of assessing the likelihood of internal erosion of embankment dams, water retaining structures and their foundations. Internal Erosion of Dams and their Foundations. Taylor & Francis Group, London, 1–23.

Fell, R, Wan CF, Cyganiewicz J, Foster M (2003) Time for development of internal erosion and piping in embankment dams. J Geotech Geoenviron 129(4):307-314.

Fox, G.A., Wilson GV, Simon A, Langendoen EJ, Akay O, and Fuchs JW (2007) Measuring streambank erosion due to groundwater seepage: correlation to bank pore water pressure, precipitation and stream stage. Earth Surface Processes and Landforms 32(10): 1558–1573.

Fox GA, Wilson GV (2010) The role of subsurface flow in hillslope and stream bank erosion: a review. Soil Science Society of America Journal, 74(3):717-733.

Fox, G.A., Felice RG, Midgley TL, Wilson GV, and Al-Madhhachi AS (2014) Laboratory soil piping and internal erosion experiments: evaluation of a soil piping model for low-compacted soils. Earth Surface Processes and Landforms 39(9): 1137–1145.

Fredlund, DG, Rahardjo H, Fredlund MD (2012) Unsaturated soil mechanics in engineering practice. Wiley, New York.

Gattinoni P, Francani V (2009) A tool for modeling slope instability triggered by piping. World Academy of Science, Engineering and Technology, 56:471-477.

Glazyrin, GY, and Reyzvikh V N (1968) Computation of the flow hydrograph for the breach of landslide lakes. Soviet Hydrology, 5: 492–496.

Hanson, GJ, Tejral RD, Hunt SL, and Temple DM (2010) Internal erosion and impact of erosion resistance. In Proceedings of the 30th US Society on Dams Annual Meeting and Conference, Sacramento, California, 773–784.

Hayashi SI, Uchida T, Okamoto A, Ishizuka T, Yamakoshi T, Morita K (2013) Countermeasures against landslide dams caused by Typhoon talas 2011. Tech Monitor, 20-26.

Hagerty, DJ (1991) Piping/sapping erosion: 1. Basic considerations. Journal of Hydraulic Engineering, 117:991–1008.

Howard AD, McLane CF (1988) Erosion of cohesionless sediment by groundwater seepage. Water Resources Research, 24(10):1659-1674.

Huggel C, Clague JJ, Korup O (2012) Is climate change responsible for changing landslide activity in high mountains? Earth Surface Processes and Landforms, 37(1):77-91.

Iverson, R.M., and Major JJ (1986) Groundwater seepage vectors and the potential for hillslope failure and debris flow mobilization. Water Resources Research 22(11): 1543–1548.

Jakob M, Lambert S (2009) Climate change effects on landslides along the southwest coast of British Columbia. Geomorphology, 107(3):275-284.

Jones, JAA (1981) The nature of soil piping: A review of research. In: Volume 3 of British Geomorphological Research Group, research monograph series. Geo Books, Norwich.

Jonkman, SN, Vrijling, JK, and Vrouwenvelder, A. C. W. M (2008) Methods for the estimation of loss of life due to floods: a literature review and a proposal for a new method. Natural Hazards, 46(3): 353–389.

Katsube K, Oguchi T (1999) Altitudinal changes in slope angle and profile curvature in the Japan Alps: A hypothesis regarding a characteristic slope angle. Geographical review of Japan, Series B., 72(1):63-72.

Korup, O. (2004) Geomorphometric characteristics of New Zealand landslide dams. Engineering Geology 73(1): 13–35.

Korup, O (2005) Geomorphic hazard assessment of landslide dams in South Westland, New Zealand: fundamental problems and approaches, Geomorphology, Vol.66(1-4), pp.167-188.

Korup O, Montgomery DR, Hewitt K (2010) Glacier and landslide feedbacks to topographic relief in the Himalayan syntaxes. Proceedings of the National Academy of Sciences, 107(12):5317-5322.

Li. T (1990) Landslide Management in the Mountain Areas of China. ICIMOD Occasional Paper no.15, International Centre for Integrated Mountain Development, Kathmandu, Nepal.

Liu, N, Zhang JX, Lin W, Cheng WY, and Chen ZY (2009) Draining Tangjiashan Barrier Lake after Wenchuan Earthquake and the flood propagation after the dam break. Science in China Series E: Technology Sciences, 52(4): 801–809.

Lobkovsky, AE, Jensen B, Kudrolli A, Rothman DH (2004) Threshold phenomena in erosion driven by subsurface flow. J Geophys Res Earth Surf 109:F04010. doi:10.1029/2004JF000172.

Maknoon, M., and Mahdi TF (2010) Experimental investigation into embankment external suffusion. Natural Hazards 54(3): 749–763.

Manville, V (2001) Techniques for evaluating the size of potential dam break floods from natural dams, Science Rep. No. 2001/28, Institute of Geological and Nuclear Sciences, Wellington, New Zealand, pp.72.

Nasrabadi, T, Ruegner H, Sirdari ZZ, Schwientek M, Grathwohl P (2016) Using total suspended solids (TSS) and turbidity as proxies for evaluation of metal transport in river water. Appl Geochem 68:1-9.

O'Connor, J.E., and Costa, J.E. (2004) The world's largest floods, past and present—their causes and magnitudes, U.S. Geological Survey Circular 1254, pp.13.

Oguchi T, Saito K, Kadomura H, Grossman M (2001) Fluvial geomorphology and paleohydrology in Japan. Geomorphology, 39(1):3-19.

Okeke, ACU, Wang F (2016a) Critical hydraulic gradients for seepage induced failure of landslide dams. Geoenvironmental Disaster. Doi: 10.1186/s40677-016-0043-z.

Okeke, ACU, Wang F (2016b) Hydro-mechanical constraints on the piping failure of landslide dams: An experimental investigation. Geoenvironmental Disaster. Doi: 10.1186/s40677-016-0038-9.

Parker GG (1964) Piping: A Geomorphic Agent in Landform Development of the Drylands. International Association of Scientific Hydrology, 65:103-113.

Peng, M, Zhan LM (2012) Breaching parameters of landslide dam. Landslides 9:13-31. doi:10.1007/s10346-011-0271-y.

Richards, KS, Reddy KR (2007) Critical appraisal of piping phenomena in earth dams. B Eng Geol Environ 66(4):381-402.

Richie, JA (1963) Earthwork tunneling and the application of soil testing procedures. J Soil Water Conserv 19:111-129.

Rinaldi, M, Casagli N (1999) Stability of streambanks formed in partially saturated soils and effects of negative pore-water pressures: The Sieve River (Italy). Geomorphology 26(4):253-277.

Rügner, H, Schwientek M, Beckingham B, Kuch B, Grathwohl P (2013) Turbidity as a proxy for total suspended solids (TSS) and particle facilitated transport in catchments. Environ Earth Sci 69(2):373-380.

Sassa K (1998) Recent urban landslide disasters in Japan and their mechanisms. In Proceedings of 2nd International Conference on Environmental Management, Australia, pp 10-13.

Sassa K (2005) Landslide disasters triggered by the 2004 Mid-Niigata Prefecture earthquake in Japan. Landslides, 2(2):135-142.

Schuster, RL (1995) Landslide dams-a worldwide phenomenon. In Proceedings of the Annual Symposium of the Japanese Landslide Society, Kansai Branch, Osaka, 1–23.

Schuster, RL (2000) Outburst debris flows from failure of natural dams, Proceedings 2nd International Conference on Debris flow Hazard Mitigation, Taipeh, pp.29-42.

Schuster, RL, Costa JE (1986) A perspective on landslide dam. In: Shuster RL (ed) Landslide dams: Processes, risk, and mitigation. Proceedings of a session in conjunction with the ASCE convention. ASCE (Geotechnical Special Publ n 3), New York, pp 1-20.

Schwarz, K, Gocht T, Grathwohl P (2011) Transport of polycyclic aromatic hydrocarbons in highly vulnerable karst systems. Environ Pollut 159:133-139.

Shrestha BB and Nakajawa H (2016) Hazard assessment of the formation and failure of the Sunkoshi landslide dam in Nepal. Natura Hazard, Vol. 82-3: 2029-2049.

Shroder, JF, Bishop MP (1998) Mass movement in the Himalaya: new insights and research directions. Geomorphology 26, 13–35.

Sidle, RC, Kitahara H, Terajima T, and Nakai Y (1995) Experimental studies on the effects of pipe flow on through flow partitioning. Journal of Hydrology 165(1): 207–219.

Singh VP, Scarlatos PD, Collins JG, Jourdan MR (1988) Breach erosion of earthfill dams (BEED) model. Natural Hazards, 1(2):161-180.

Stefanelli CT, Catani F, Casagli N (2015) Geomorphological investigations on landslide dams. Geoenvironment Disasters 2015; 2(1):21.

Storm, A. (2013) Geological prerequisites for landslide dams' disaster assessment and mitigation in central Asia. In: Wang F, Miyajima M, Li T, Shan W, Fathani T (eds) Progress of geo-disaster mitigation technology in Asia. Environmental Science and Engineering (Environmental Engineering). Springer, Berlin, pp 17-53.

Stubblefield, AP, Reuter JE, Dahlgren RA, Goldman CR (2007) Use of turbidometry to characterize suspended sediment and phosphorus fluxes in the Lake Tahoe basin, California, USA. Hydrol Process, 21:281-291. doi:10.1002/hyp.6234.

Swanson, FJ, Ouyagi N, and Tominaga M (1986) Landslide dams in Japan, in Schuster, R. L., Landslide Dams: Process, Risk and Mitigation: ASCE Geotechnical Special Publication, No.3, pp.131-145, 1986.

Tacconi, C, Vilímek V, Emmer A, Catani F (2018) Morphological analysis and features of the landslide dams in the Cordillera Blanca. Landslides, 15, 3, 507-521.

Takahashi, T (1991) Debris flow, Monograph Series of IAHR, Balkema, pp.1-165, 1991.

Takaji, K, Yusuke F (2008) Effect of particle gradation on seepage failure in granular soils. In: Sekiguchi, Hideo (ed.): Proceedings of the 4th international conference on scour and erosion (ICSE-4), November 5-7, 2008. The Japanese Geotechnical Society, Tokyo, Japan. pp 497-504.

Uhlir, CF (1998) Landslide-dammed lakes: a case study of the Lamabagr and Chanurikharka landslide deposits, Dolakha and Solukhumbu districts, eastern Nepal, Journal of Nepal Geological Society, Vol. 18, pp.329-334.

Wang, F, Dai Z, Okeke CAU, Mitani Y, Yang H (2018) Experimental study to identify premonitory factors of landslide dam failures. Engineering Geology 232:123-134.

Wang HB, Sassa K, Xu WY (2007) Analysis of a spatial distribution of landslides triggered by the 2004 Chuetsu earthquakes of Niigata Prefecture, Japan. Natural Hazards, 41(1):43-60.

Wilson, G (2011) Understanding soil-pipe flow and its role in ephemeral gully erosion. Hydrological Processes 25(15): 2354–2364.

Wilson, GV, Periketi RK, Fox GA, Dabney SM, Shields FD, Cullum RF (2007) Soil properties controlling seepage erosion contributions to streambank failure. Earth Surface Processes and Landforms, 32(3):447-459.

Wilson, GV (2009) Mechanisms of ephemeral gully erosion caused by constant flow through a continuous soil-pipe. Earth Surface Processes and Landforms 34(14): 1858–1866.

Wit, JD, Sellmeijer JB, and Penning A (1981) Laboratory testing on piping, 517–520. In: Tenth International Conference on Soil Mechanics and Foundation Engineering.

Xu Q, Fan XM, Huang RQ (2009) Landslide dams triggered by the Wenchuan Earthquake, Sichuan Province, Southwest China. Bulletin of Engineering Geology and the Environment.

Zhang LM, Chen Q (2006) Seepage failure mechanism of the Gouhou rockfill dam during reservoir water infiltration. Soils and Foundations, 46(5):557-568.

Annexes

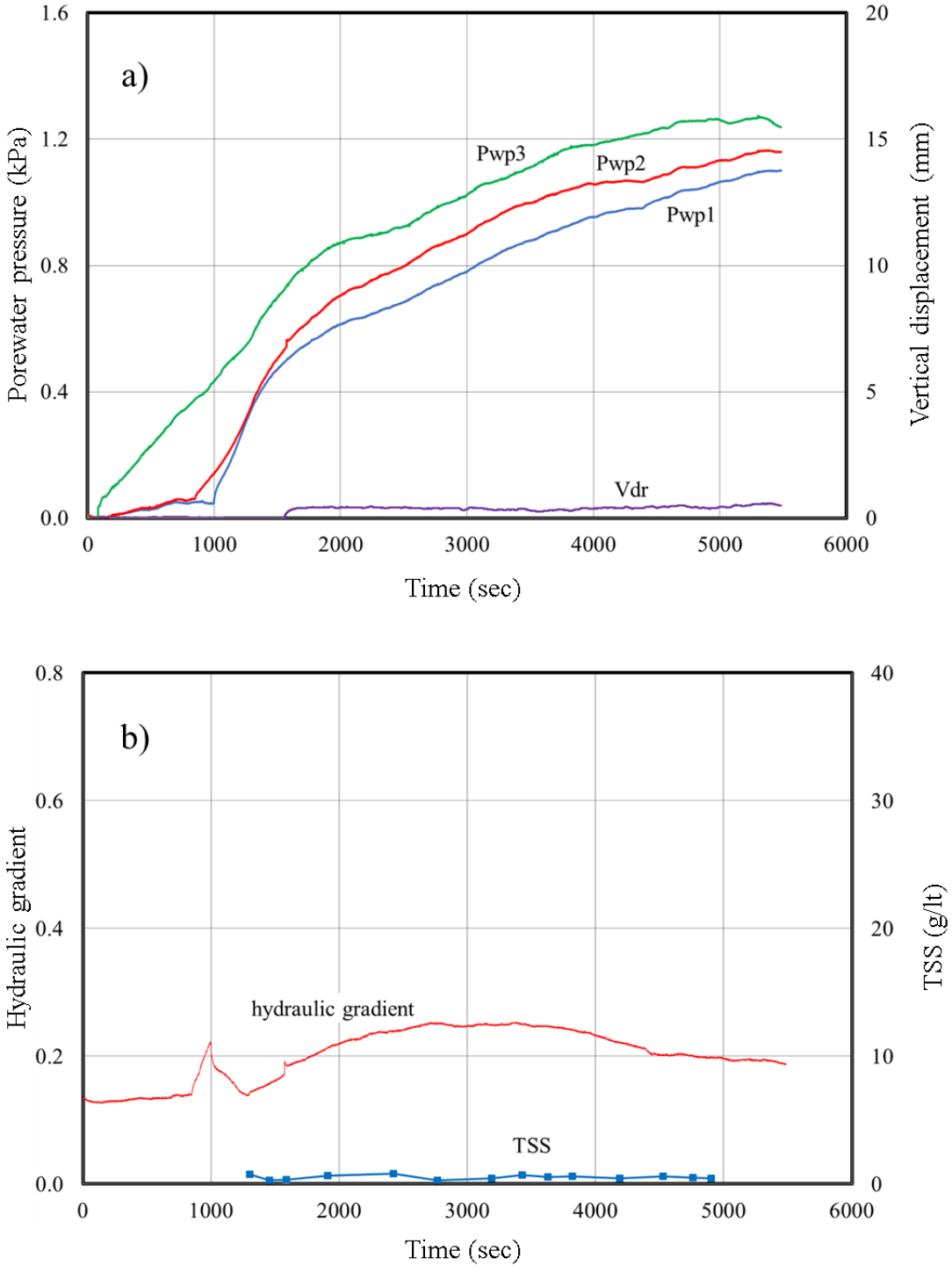

Fig 8.1 Experiment results of experiment No. EXP 6NF of GIII sample. a) Pore water pressure and vertical displacement curves; b) Hydraulic gradient and TSS

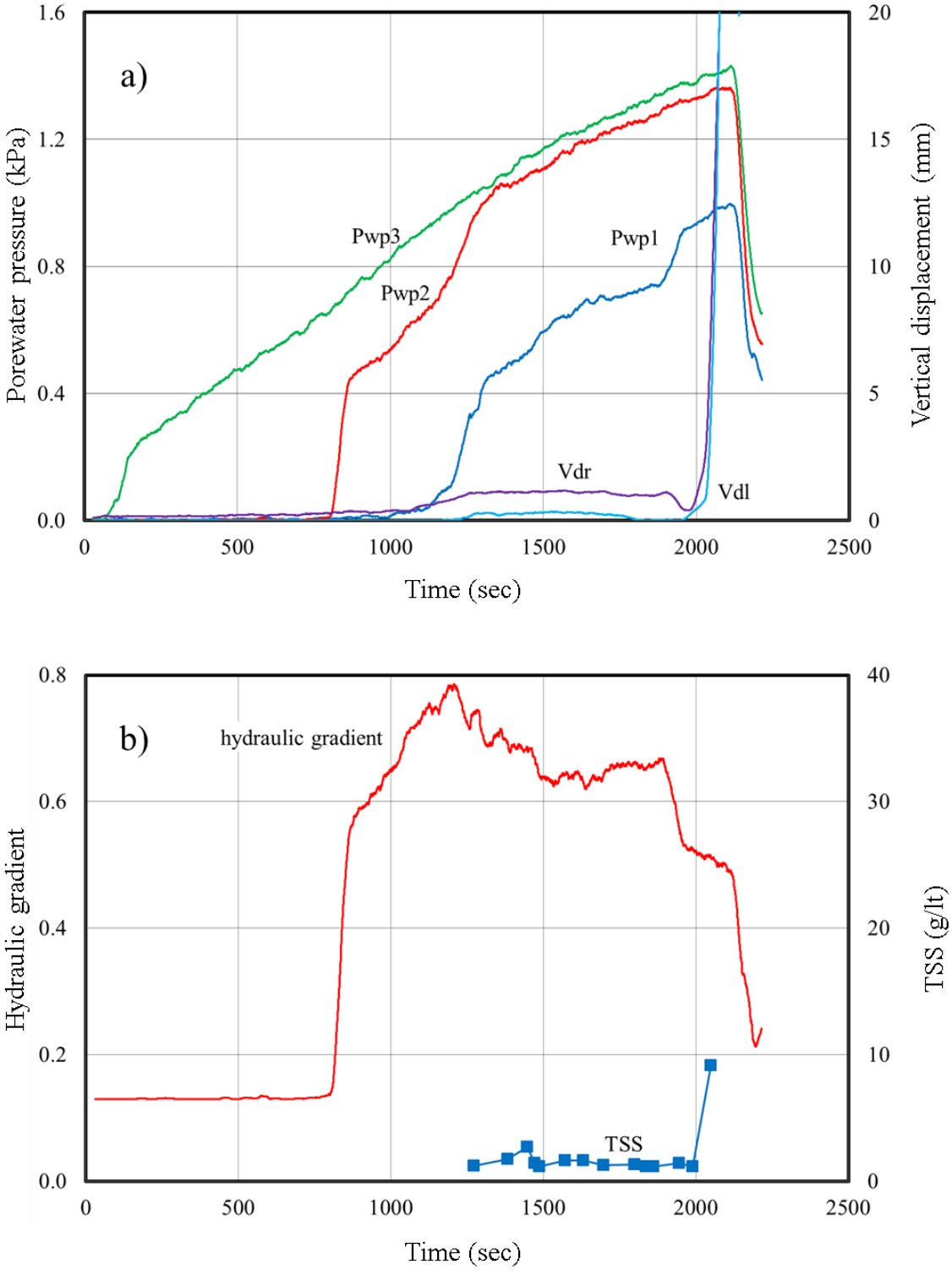

Fig. 8.2 Experiment results of experiment No. EXP 3F of GIII sample. a) Pore water pressure and vertical displacement curves; b) Hydraulic gradient and TSS

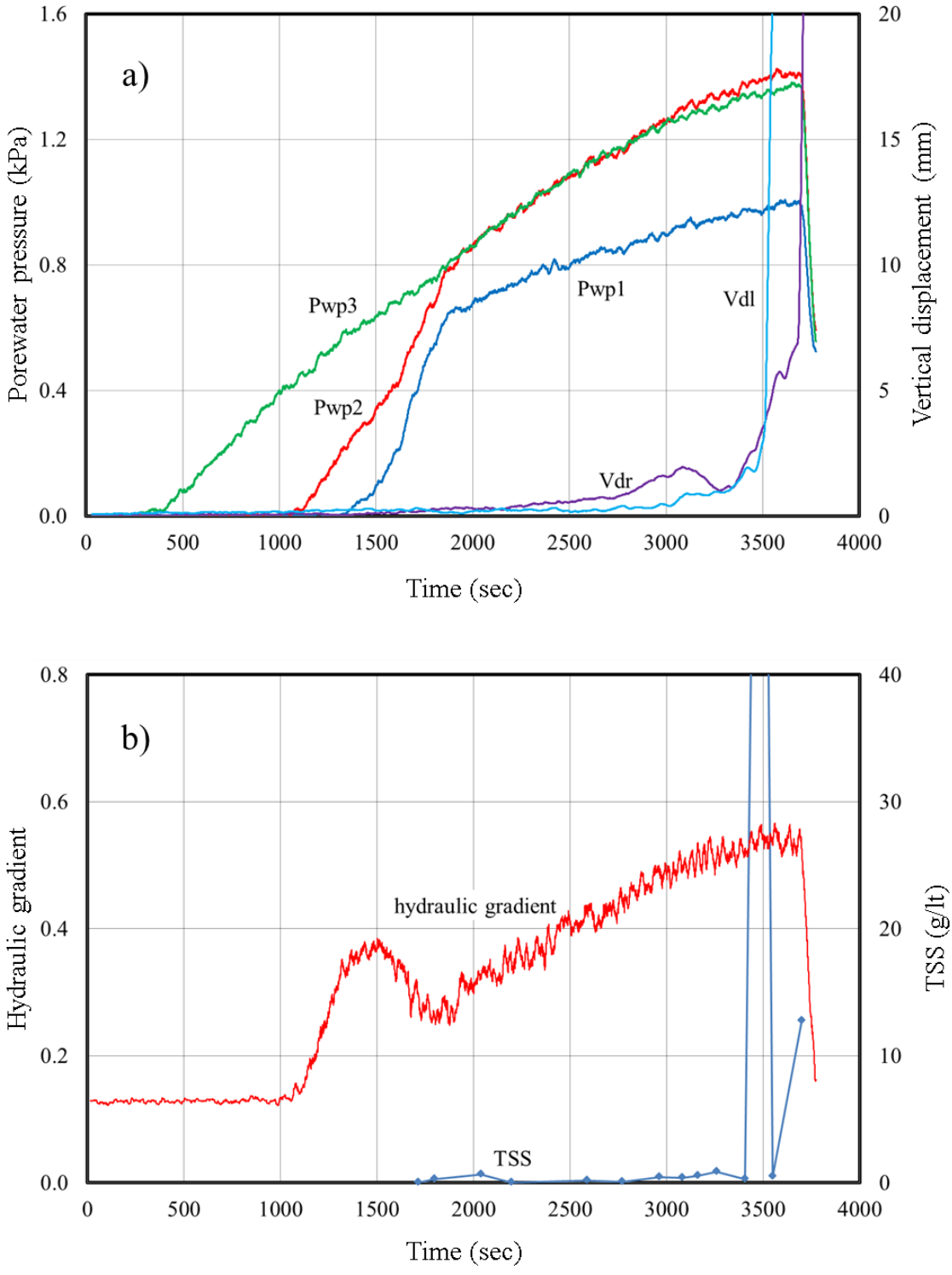

Fig. 8.3 Experiment results experiment No. EXP 5F2, of GIII sample. a) Pore water pressure and vertical displacement curves; b) Hydraulic gradient and TSS

a)

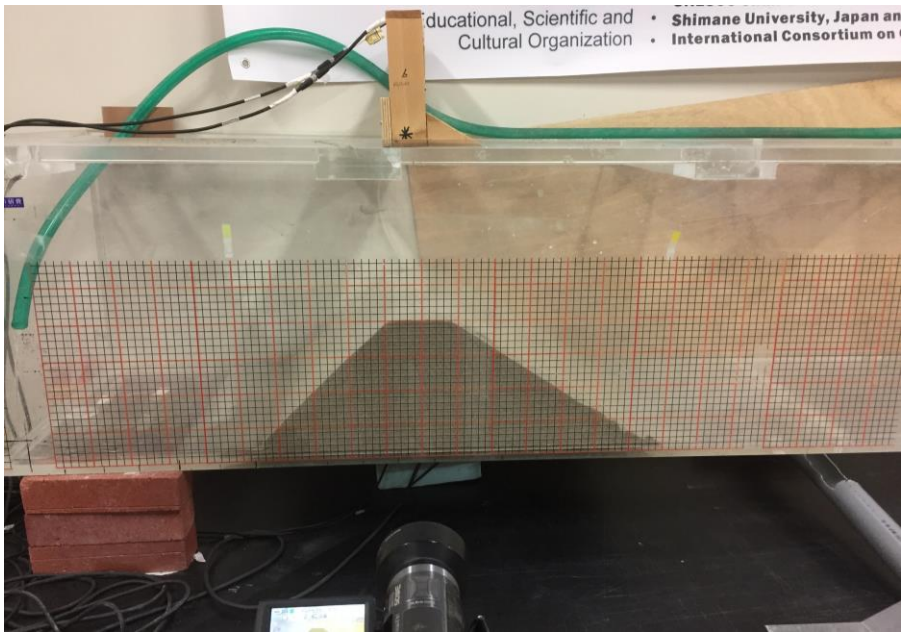

b)

Fig. 8.4 Photographs of experimental setup. a) Side view of flume tank during experiment; b) Downstream slope of dam with laser sensor at the top of flume tank